(2)

R+D. 5180-EE-01

QUANTUM PHENOMENA IN SEMICONDUCTOR STRUCTURES

Dr M Pepper
Cavendish Laboratory, University of Cambridge
Madingley Road, Cambridge CB3 OHE
United Kingdom

Contract: DAJA-85-C-0045

FIRST ANNUAL REPORT : OCTOBER 1985 - OCTOBER 1986

Interim rept no. 2, Oct 85 - Apr 86
Interim rept nos. 4, 5 + 6, Oct 86 - Apr 88

The Research reported in this document has been made possible through the support and sponsorship of the U.S. Government through its European Research Office of the U.S. Army.

~~This report is intended only for the internal management use of the Contractor and the U.S. Government.~~

88 6 6 191

1. THE USE OF LITHOGRAPHY TO PRODUCE ONE DIMENSIONAL STRUCTURES

We have commenced experiments aimed at producing a metal pattern on the AlGaAs of an AlGaAs-GaAs modulation doped heterojunction. This will enable us to investigate details of the transport when the effective sample length is considerably less than the scattering mean free path.

Many of the proposed experiments of this grant concern one dimensional effects and we have concentrated (during this last period) on the energy levels in narrow modulation doped electron channels in AlGaAs-GaAs heterojunctions. Previously we demonstrated the existence of disorder-induced, one-dimensional conductivity corrections in a narrow-channel electron gas within a split-gate GaAs:AlGaAs heterojunction field-effect transistor. At temperatures such that the phase-relaxation (inelastic) length and the interaction length are greater than the channel width, the quantum corrections to the conductivity become one dimensional.

We have now investigated the effects of a large, transverse, magnetic field on the conductivity when the channel is narrow. A WKB calculation was performed which shows that a magnetic-field-induced depopulation of the one-dimensional subbands occurs. The mobility in this system is much higher than in other quasi 1D systems so that lifetime broadening of electronic subbands ($\equiv h/\tau$) is sufficiently small for subband depopulation to be directly observed as structure in the magnetoconductance. Here τ is the elastic lifetime.

The devices used in this work had a split gate separation of 1.0 μm. The channel width was extracted from the positive magnetoconductance arising from quantum interference effects. The quantum interference is quenched by a weak magnetic field when the cyclotron length is shorter than the elastic mean free path, leaving only the conductivity correction due to the electron-electron interaction given by

$$\delta G = - (e^2\alpha/\pi h) (\hbar D/2kT)^{1/2} \qquad (1)$$

where α is the 1D interaction parameter and has the value 1.33, and D is the electron diffusion coefficient. The screening parameter F has the value of 0.35 in this range. The exchange contribution dominates over the Hartree contribution and hence α does not vary signficantly with r change in F or carrier concentration.

For channel widths greater than 1000 Å the value of $\delta G(B)/G(B = O)$ is so small that the channel width cannot be accurately determined from the quantum inteference corrections. However, the width can be independently determined from the temperature-dependent electron-electron interaction correction. In these devices a transverse magnetic field of 0.15 T was

sufficient to quench the quantum interference without enhancing the interaction correction ($|g_L \mu B| << kT$, where g_L is the Landé g factor and μ is the Bohr magneton), so that the change in the conductivity with temperature depends only upon the electron-electron interaction according to Eq. (1).

The conductance g (G/L, where L is the channel length) was measured in a magnetic field of 0.15 T as a function of temperature and plotted against $T^{-1/2}$. D was determined from the best straight-line fit. Extrapolation to $T^{-1/2}=0$ gave a value for the Boltzmann conductance given by $g_B = N(E_F)De^2t/L$. If we assume a 2D density of states $N(E_F)$ and use the estimate of D obtained from the gradient it is possible to extract the channel width t. The assumption of a 2D density of states is a good approximation for widths greater than 1000Å when several (i.e., more than four) subbands are occupied.

The magnetoconductance for different channel widths was measured in the temperature range 4.2 to 0.35 K in magnetic fields up to 8 T. The magnetic field strength B was measured with a calibrated Hall probe with a nonlinear response above 1 T. In order to avoid electron heating, the electric field along the channel under the gate was less than 1V/m and the conductivity was measured by conventional phase-sensitive techniques.

When the narrow-channel resistance is not totally dominant ($V_g > -3.0$ V), the magnetoconductance exhibits two Fourier components. One component corresponds to a carrier concentration of 4.0×10^{11} cm^{-2} and arises from Shubnikov-de Haas oscillations in the 2D regions between the channel and the source and drain. The other component has a larger period and is due to Shubnikov-de Haas oscillations within the channel itself. The period of these oscillations did not vary as the width was reduced from 10000 to 2500 Å showing that the carrier concentration within the channel remained constant at $(1.5 \pm 0.1) \times 10^{11}$cm^{-2}. The origin of the drop in carrier concentration may be the electron-beam lithography. In the calculations performed we have assumed this concentration for all channel widths.

In order to illustrate the general behaviour of the magnetoconductance of the channel as a function of confining voltage we plotted a fan diagram. We first point out that as the effective sample aspect ratio is always less than $^1/30$ (length - 15 μm width less than 5000 Å), the maxima in conductance correspond to E_F lying between Landau levels and hence the fan passes through zero index. The initial decrease in V_G produces no change and the experimental points are coincident. Reduction in the channel width below 2500 Å produces a change in slope and a pronounced curvature from 1/B behaviour at low values of magnetic field which becomes stronger

with decreasing width (plotting minima in conductance also gives the same behaviour).

This behaviour arises as the perturbation to the Landau levels is not weak and the magnetoconductance oscillations are no longer periodic in 1/B (an effect which is most significant at low B), but arise from the successive magnetic depopulation of one-dimensional hybrid electric-magnetic subbands. The effects of a parallel magnetic field on the depopulation of quantized levels in a 2D system is well known. In the present experiment the narrow width of the channel gives rise to 1D subbands and these are forced through the Fermi level by an increasing transverse magnetic field. As each level passes through the Fermi level a sharp change occurs in both the density of states and intersubband scattering, which, in an ideal system, results in a discontinuity in the conductance. We have calculated the magnetic depopulation of the subbands and find good agreement between experiment and theory. These results are still preliminary and a more detailed comparison will be reported in the next report.

We have investigated localisation and interaction effects on transport in GaAs-AlGaAs heterojunctions when the 2D electron gas is progressively narrowed in the manner previously described. The negative magneto-resistance arising from the suppression of quantum interference has shown that one dimensional behaviour is obtained when the channel is less than about 2000Å width. The inelastic scattering is found to be due to interaction of electrons with fluctuations in charge density. This finding is in agreement with recent theories suggesting that this mechanism dominates in 1D, whereas it is weaker in 2D and 3D.

2. SHORT CHANNEL DEVICES

Transport through the depleted region under the gate of a GaAs-AlGaAs heterojunction FET has been investigated. Experiments have shown that phonon emission by hot electrons can be observed, indicating that energy loss via acoustic phonons is not totally effective and some electrons travel ballistically. Work is continuing on this topic.

3. FUTURE WORK

This will include experiments on phonon emission as a function of dimensionality, the samples for which are now ready and interference effects in heterojunction loops. In addition, further studies of macroscopic quantum effects in small structures will be performed during the coming year.

M Pepper

October 1986

Quantum Phenomena in Semiconductor Structures

Dr M Pepper

Cavendish Laboratory

University of Cambridge

Madingley Road

Cambridge CB3 OHE

United Kingdom

Contract: DAJA-85-C-0045

Second Interim Report

October, 1985 - April, 1986

The Research reported in this document has been made possible through the support and sponsorship of the U.S Government through its European Research Office of the U.S. Army. This report is intended only for the internal management use of the Contractor and the U.S. Government.

Experiments have been carried out on transport in GaAs-AlGaAs heterojunctions when the 2D electron gas is progressively narrowed. The narrowing is accomplished by the action of a Schottky gate; investigations of the negative magneto-resistance arising from the suppression of quantum interference have shown that one dimensional behaviour is obtained when the channel is less than about 2000Å width. The inelastic scattering is found to be due to interaction of electrons with fluctuations in charge density. This finding is in agreement with recent theories suggesting that this mechanism dominates in 1D, whereas it is weaker in 2D and 3D.

The effects of a magnetic field on 1D transport have been investigated. It has been found that the magnetic field forces the quantised 1D sub-bands through the Fermi energy giving conductivity oscillations in the shape of spikes. These results are being compared with a theory we are developing.

Work has continued on the magneto-phonon effect in lightly doped GaAs Schottky gate FET's. A shift in the position of the resonance as the channel is narrowed has not yet been observed; different values of doping are now being used in an attempt to observe the effect.

Transport through the depleted region under the gate of a GaAs-AlGaAs heterojunction FET has been investigated. Experiments, which are continuing, have shown that phonon emission by hot elcctrons can be observed, indicating that energy loss via acoustic phonons is not totally effective and some electrons travel ballistically. Work is continuing on this topic. Experiments which will be performed during the next period of the grant will include macroscopic quantum phenomena, in particular quantum coherence and the quantum Hall effect.

Quantum Phenomena in Semiconductor Structures

Dr M Pepper

Cavendish Laboratory

University of Cambridge

Madingley Road

Cambridge CB3 OHE

Contract: DAJA-85-C-0045

Fourth Interim Report

October, 1986 - April, 1987

The research reported in this document has been made possible through the support and sponsorship of the US Government through its European Research Office of the US Army.

Introduction

This report contains a description of our work on the use of Gallium Arsenide FET's for the investigation of phonons. The technique adopted was the magneto-phonon effect and a new geometrical effect was found which illustrates how device geometry affects the results.

Experiments on the Magneto-Phonon Effect in GaAs Devices

1. INTRODUCTION

The magnetophonon effect was first predicted by Gurevich and Firsov in InSb and detected in the magnetoresistance of n-type InSb at about liquid nitrogen temperatures by Puri and Geballe in 1963. It consists of small oscillations periodic in 1/B superimposed on the usual smooth increase in resistance of a semiconductor with increasing magnetic field (figure 1).

In a strong magnetic field the allowed energies of electrons becomes

$$E^2{}_n k_z = \frac{\hbar^2 k_z^2}{2m^*} + (n+1/2)\hbar\omega_c$$

where ω_c is the cyclotron frequency, equal to eB/m*, and k_z is the wavevector along the magnetic field direction.

This corresponds to the motion parallel to the field being unaffected while motion perpendicular to the field is circular. Quantisation of angular momentum leads to the radii of the orbits taking only the values

$$r_c = \left(\frac{2\hbar(n+1/2)}{eB} \right)^{0.5}, \quad n = 0, 1, 2, \ldots$$

This quantity is the cyclotron radius. The energy of perpendicular motion is also quantised, as above, into equally spaced levels $\hbar\omega_c$ apart. Because the density of states is inversely proportional to dE/dk, which is zero at k=o, the density of states has periodic singularities. Most electrons thus have energies corresponding to one of these singularities, and these energies are known as Landau levels. They are equally spaced and their separation is proportional to the magnetic field intensity.

The E versus k curve for longitudinal optic phonons is very flat. In fact by the time it intersects the curve for electrons the energy differs from that at the zone centre by less than one part in 10^5. This means that it is possible to speak of a single energy for the LO phonons with the range of wavevectors that can be absorbed or emitted by an electron. This energy corresponds to a temperature of about 400 Kelvin in GaAs, so the number of optic phonons present varies very rapidly with temperature, for instance increasing by a factor of about 60 between 50 and 100 Kelvin. This increase is generally sufficient for optic phonon scattering to begin to dominate the electrical resistance somewhere in this temperature range.

When the separation between Landau levels is equal to the LO phonon energy the probability of absorption or emission of an LO phonon increases, since this rate is proportional to the product of the initial and final densities of states, which are both now very large. The same will happen whether the LO phonon energy is equal to the separation between one, two or more Landau levels. Hence the condition for this additional scattering is that

$$n\hbar\omega_c = \hbar\omega_p$$

or equivalently

$$\frac{1}{B} = \frac{n.e}{m^*.\omega_p}$$

showing that the resistance changes from the additional scattering are periodic in 1/B.
A density of states exactly as in figure 2 would produce infinite values of resistance at the resonances. In practice the resistance change is never more than about 10%, and is often very much less. The reason for this is the loss of the singularities in the density of states, the peaks of which are smeared out by approximately the amount of h divided by the finite time an electron spends in a state before being scattered.

The amplitude of the oscillations is found to vary with temperature, sample purity and magnetic field (or equivalently with the index number n of the peak). The optimum temperature to observe the magnetophonon effect is usually about 150 Kelvin; at low temperatures there will be very few LO phonons with which the electrons can interact, even when the resonance condition is satisfied, and at high temperatures, though most of the scattering is by optic phonons, it is so rapid that the sharp peaks in the density of states are destroyed.

The ratio of the amplitudes of the oscillations in different samples is similar at all temperatures, and the amplitudes are inversely proportional to each sample's concentration of ionised impurities. Hence, rather surprisingly, the temperature and impurity variations of the amplitude of a given peak can be separated. Figure 1, 3, 4 illustrates this.

It is found empirically that the variation with magnetic field of the oscillatory part of the magnetoresistance is well represented by

$$\Delta\rho / \rho_0 = C \times \exp(-\Gamma\omega_p/\omega_c) \quad \times \quad \cos(2\pi\omega_p/\omega\, c),$$

so that the amplitude of the nth peak is proportional to $\exp(-\Gamma n)$. Γ is a function of both temperature and impurity concentration. Conditions that make C small also tend to increase Γ, so that oscillations which are weak initially also disappear more rapidly as the magnetic field is reduced. Barker (1970) has a successful theory of the amplitude variations which produces the above expression as the first and largest term of a harmonic series. In his theory Γ is the imaginary part of the electron self energy arising from both impurity and optic phonon scattering.

The above discussion applies when B is perpendicular to j. The peaks in the density of states occur at $k_z=0$, so electrons moving between states in these peaks change their momentum along the direction of B very little. If this is also the direction of current flow the additional scattering will have little effect on the current. Hence the magnetophonon effect is very weak for B parallel to j, and second order effects involving a second phonon or an impurity are important. These lead to minima rather than maxima in resistance, and these minima may be shifted away from the resonance fields.

Hot electron conditions

Magnetophonon oscillations can be observed even at very low lattice temperatures if an electric field is applied that is large enough to heat the electron gas by a few Kelvin. The electrons generally exchange energy amongst themselves rapidly enough to establish a nearly Maxwellian energy distribution. At low lattice temperatures the mobility of the electron gas is determined by ionized impurity scattering, which varies inversely with temperature, but most of the energy loss from the electron gas is through the emission of optic phonons by the electrons in the high energy tail of the energy distribution. The emission probability is enhanced at the magnetophonon resonances and so the whole electron gas is cooled. Resistance maxima occur at the resonance fields because of the lowered electron temperature and the ionized impurity scattering. In some 3 - 5 semiconductors other than GaAs distortions of the energy distribution form a Maxwellian form are important and this is not the case. Because of the way in which these oscillations arise the size and sign of the resistance changes are now almost independent of the direction of B relative to the current.

2. MAGNETOPHONON OSCILLATIONS IN GaAs FIELD EFFECT TRANSISTORS

Device strucure and fabrication

Two designs of device were used. The first was a Hall bar with length 750μm, width 115μm and four equally spaced sidearms per side, and a 20μm (gate length 10μm) device 600μm wide. These will be referred to as long and short devices.

Isolation was achieved by etching away the active layer surrounding each device. Bonding pads would normally be deposited on the substrate exposed by this process, and metallisation run up the sides of the device "mesa" to make contact to the correct region. Since many of the layers used had active layers many microns thick, problems were encountered in achieving continuous metallisation over the large step at the edge of the mesa. This was overcome by extending the mesa to include the bonding pads and matallisation regions also.

The very high mobility layers wre grown by our industrial collaborators in a hydride VPE machine. This grew excellent material but was not set up with p-type dopants. It was found to be impossible to grow a low-doped n-type layer on a normal p-type substrate with this machine, apparently

because of an autodoping effect. When a back gate was required thus iproblem was overcome by growing a p-type layer on a semi-insulating substrate in a MOCVD reactor, then transferring this to the hydride VPE reactor to grow the active layer after an in-situ etch.

TABLE 1 - Summary of Layers

Layer	N doping	Depth	Substrate	77K mobiliy
MV73	$2x10^{14}cm^{-3}$	6.0µm	semi-insulating	$6\ m^2v^{-1}sec^{-1}$
B257	$2x10^{14}cm^{-3}$	5.0µm	semi-insulating	14
B977	$4x10^{14}cm^{-3}$	5.0µm	p on si	7
B1987	$2x10^{15}cm^{-3}$	3.2µn	p on si	-
B1988	$6x10^{15}cm^{-3}$	4.0µm	p on si	-
B1220	$2x10^{16}cm^{-3}$	1.5µm	p	-
B1218	$6x10^{16}cm^{-3}$	0.4µn	p	-

Device Operation

Both the metal gate and the p-type layer initially contain unoccupied states with lower energies than those in the n-type active layer. Electrons from the active layer then move into these states, leaving behind regions depleted of free electrons and hence with a net positive charge. This continues until the dipoles created by this charge movement produce a potential barrier large enough to prevent further transfer. By biassing the gates negatiavely with respect to the source thee depletion regions can be extended, reducing the conductivity between the source and drain by narrowing the conducting channel connecting them. If a positive voltage is applied to the drain to produce a source to drain current, the depletion regions will constrict the channel more near the drain as the gate to channel potential is greater there. If the drain voltage is large the depletion regions will meet somewhere near the drain end of the channel. Current will continue to flow as electrons are injected into the depletion region from the channel, but the current is now nearly independent of the drain voltage, since increasing it only moves the point of intersection of the depletion regions slowly nearer to the source, affecting the field in the undepleted region only a little (assuming L>>d). This is the usual operating condition of the device, but for the experiments described later very small drain voltages were used so that the channel width was nearly uniform and the source -

drain current obeyed Ohm's law, with the resistance determined by the gate voltage.

A simple expression for the source - drain conductivity can be obtained by making the following assumptions:

The channel doping level N_d is constant.

The electron mobility is constant.

The depletion regions have zero free electron concentration, but this rises immediately to N_d at the edges. This is called the depletion approximation.

Integration of Poisson's equation shows that the potential change across a depletion region of length l is $l^2 N_d e/2\,\varepsilon$. Equating this to the gate to source voltage, Vg, the proportion of the channel remaining undepleted is

$$1 - \left[\frac{V_g}{V_p}\right]^{0.5}$$

where V_p is the "pinch-off" voltage, defined by

$$V_p = \frac{d^2 e\, N_d}{8\varepsilon}$$

The channel conductivity is proportional to this. The contact potentials between the gates and active layer are of the order of a volt and must be added to the externally applied bias to determine V_g.

The depletion approximation will be poor when the thickness of the channel remaining undepleted is less than the thermal blurring of the edges of the depletion regions. The Debye length, defined as

$$L_D = \left[\frac{\varepsilon KT}{e^2 N_d}\right]^{\frac{1}{2}}$$

is a measure of this blurring, L_d is the distance into a depletion region at which the potential energy of an electron has risen by 0.5 KT. In the limit of gate voltages, much greater than V_p there will be too few electrons to appreciably affect the potential, which is therefore given by $x^2 KT/2L_D{}^2$.

where x is the distance from the centre of the channel. The electron concentration will vary as $N_e exp - (_x^2/2L^2_D)$ because of this increasing potential. The number of electrons per unit area is then $N_e.L_D.(2\pi)^{0.5}$, so the electron distribution has an effective width of $L_D.(2\pi)^{0.5}$, ~ 2.5 L_D. In addition, because there are too few electrons for screening to occur, the potential in all parts of the active layer will follow changes in the gate potential and the electron concentration will vary throughout as $exp(-eV_g/KT)$. This region in which the number of electrons varies exponentially with gate voltage is called the subthreshold region. In the transition region between thicknesses much larger than L_D and the subthreshold region and the electron distribution if required can be found by numerical integration.

3. Experimental Results and Discussion

Many combinations of doping level, device geometry, temperature and relative orientation of device, current and magnetic field are possible. These have been grouped according to the results obtained. Results for B perpendicular to j will be considered first.

Long devices, B parallel to layer

In this configuration the results were the same as for bulk samples: With all materials resistance maxima occurred at the fields expected for magnetophonon resonance. The relative amplitudes of oscillation were in the same order as the 77K mobilities. The temperature dependence of the oscillation amplitude was as expected for ohmic conditions and is shown for a B257 device in figure 4.

Long devices, B perpendicular to layer

With most materials similar results to those above were obtained, but with B257, the highest mobility material, the oscillations were much smaller and became inverted above a magnetic field of about 5 tesla (figure 5).

Short devices

These showed minima in resistance at resonance for B perpendicular to the layer but maxima for B parallel to the layer (figure 5).

DISCUSSION

Figure 6 defines some symbols used in this section. In a long sample the ratio of voltage to current

is proportional to ρ_{xx}, but in a short sample it is proportional to $1/\rho_{xx}$.

This can be seen as follows:

$$j_x = \sigma_{xx}.E_x + \sigma_{xy}.E_y$$

A short sample will have its Hall voltage shorted out by the low resistance ohmic contacts at each end, so that $E_y = O$.

Hence

$$\frac{V}{I} = \frac{L\,E_x}{w\,t\,j_x} = \frac{L}{w\,t} \times \frac{1}{\sigma_{xx}}$$

Since σ and ρ are inverse tensors,

$$\frac{1}{\sigma_{xx}} = \rho_{xx} + \frac{(\rho xy)^2}{\rho_{xx}}$$

ρ_{xy} is zero with no magnetic field, but from the simplest theory of the Hall effect with a magnetic field in the z direction ρ_{xy} is given by B/(n.e), where n is the concentration of electrons. Hence

$$R(B) = \frac{L}{w.t}\left[\rho_{xx}(B) + \left[\frac{B}{n.e}\right]^2 \times \frac{1}{\rho_{xx}(B)}\right]$$

For small values of B, R will be proportional to ρ_{xx} and show maxima at magnetophonon resonance, and for large values of B, R varies as $1/\rho_{xx}$ and will show minima. Minima always occur at fields large enough to observe magnetophonon oscillations.

A long device will have end regions in which the Hall voltage is shorted and a central region in which it is not. The magnetophonon oscillations in these regions will be out of phase and may almost cancel. Changes between maxima and minima at resonance can occur if the amplitudes of

oscillation in the two regions do not vary identically with B.

The length of the region at each end of the device in which the Hall voltage is shorted will be similar to the channel width w. This can be seen from figure 6: the length of the "short circuit" path through the end contact is about k. For k >> w the "short circuit" path will have a higher resistance than the region between A and B across which the Hall voltage is developed and so will have little effect, also conversely. The results therefore depend on the length to width ratio of the device seen along the direction of B - if this is large a small proportion only of the device will have its Hall voltage shorted and resistance maxima will occur at resonance, and vice versa.

The results, summarised below, are in accordance with these ideas.

Configuration	Aspect ratio	Result
Long, B∥layer	375	Maxima, $\Delta R/R = 3\%$
Short, B∥layer	~10	Maxima, $\Delta R/R = 1.5\%$
Long, B⊥layer	7	Inverts B 5T. $\Delta R/R = 0.1\%$
Short, B⊥layer	~0.03	Minima, $\Delta R/R = -1.5\%$

The following simple calculation demonstrates that this effect is the appropriate size. Consider the model of the device illustrated in figure 6. The Hall voltage is assumed to be completely shorted within the regions of length k/2 and unaffected in the central region. From this,

$$R = \frac{k}{w.t} \times \frac{1}{\sigma_{xx}} + \frac{(L-k)}{w.t} \times \rho_{xx}$$

$$= \frac{L}{w.t} \left[\rho_{xx} + \frac{k}{L} \left[\frac{B}{n.e} \right] \times \frac{1}{\rho_{xx}} \right]$$

from which

$$\frac{dR}{d\rho xx} = \frac{L}{w.t}\left[1 - \frac{k}{L}\left[\frac{B}{n.e}\right]^2 x \left[\frac{L}{\rho_{xx}}\right]^2\right] = \frac{L}{w.t}\left[1 - \frac{k}{L}[\mu B]^2\right]$$

where

$$\mu = \frac{1}{n.e.\rho_{xx}}$$

and is the drift mobility.

The condition for the oscillations to invert is that this derivative is zero

i.e. $\mu B = \sqrt{(L/k)}$

somewhere in the range of interest. This depends on the aspect ratio and mobility of the device. μB can be found from the Hall voltage between opposite sidearms of a long device;

$$\mu B = \frac{E_y}{E_x} = \frac{L V_h}{w V_t}$$

L/k can be found from the ratio of the voltage between adjacent sidearms to the voltage across the whole device:

$$V_s = I \times \frac{l}{w.t} \times \rho_{xx},$$ (l is the distance between adjacent sidearms)

$$V_t = I \times \frac{L}{w.t} \times \rho_{xx} \times \left[1 + \frac{k}{L}(\mu B)^2\right]$$

The last term arises from the extra magnetoresistance of the region in which the Hall voltage is shorted. Hence

$$\frac{L}{k} = L\left[\mu B\right]^2 x \left[\frac{V_s}{lV_t - LV_s}\right]$$

The calculated value of L/k is 19.6 at B = 3 tesla and 19.7 at 6 tesla. The constancy of this figure suggests that the model works fairly well. L/k = 19.6 means that k/w = 0.35, which is of order 1 as would be expected. Equating the expressions for $(\mu B)^2$ and L/k shows that th criterion for oscillations to invert is equivalent to

$$V_t = \frac{2V_s.L}{l}$$

For the long devices L/l = 5. Figure 7 shows V_t and $10.V_s$ on the same axes. They intersect at B = 3.8, whereas inversion was found at B = 5.5. This estimate can be improved by taking into account contact resistance, which will cause the channel voltage to be less than V_t. At B = O , V_t was about 20% greater than 5 x V_S. There is also a slight difference in temperature between the two curves of figure 7.

These ideas can be checked experimentally by using the side contacts of the device. A constant current was passed down a long device and the magnetophonon oscillations appearing between adjacent pairs of contacts are shown in figure 8, scaled so that the total voltage across the device can be found by adding them as they are drawn. It can be seen that the oscillations in the end regions are out of phase with those in the centre and increase more rapidly with B, eventually becoming large enough to change the phase of the total.

This explanation also explains the data of figure 9, in which the oscillation amplitude in a short device with B parallel to the layer at first increases as the conducting channel is narrowed by application of a negative gate voltage. In this case the aspect ratio is sufficient to prevent inversion, but the amplitude is noticeably reduced. Narrowing the conduction channel will increase the aspect ratio and prevent this.

B parallel to j

Minima in resistance near the resonant field occured. With long devices these minima were shifted to fields about 3% lower than the resonant fields, but no such shift was apparent with the short devices. Other differences are that the oscillation amplitude was much greater in the short devices, and the ratio of the resistance at 6 Tesla to that at 3 Tesla was 2.8, compared to only 1.2 under similar conditions for the long devices. One explanation for this is that in the short devices the gate occupies only 1/2 of the distance between the source and drain, and the depletion region below it is a large proportion of the layer depth. This means that there is a significant component of the current perpendicular to the layer. The interaction of this with the magnetic field will produce a Hall voltage across the 600μm. dimension of the device, which will be shorted by the contacts, as with B perpendicular to both layer and current producing large magnetoresistance and large, inverted oscillations at the resonant fields.

Hot electron oscillations

By applying large electric fields (above 5×10^3 Vm^{-1}) it was possible to observe magnetophonon oscillations in MV73 devices even at low temperatures. The field required was appreciably greater for B perpendicular to j compared with B parallel to j, presumably because of the extra magnetoresistance. At low temperatures the "impurity series" oscillations were observed where an electron falls from a Landau level to an impurity level. These were used to check that the Hall probe used for magnetic field measurements had been correctly calibrated. This calibration was carried out by measuring the positions of normal, ohmic magnetophonon oscillations in a wide variety of devices. These agreed well with each other, but some uncertainty remained because of the difficulty of deciding which experimentally observed peak corresponds to which resonance and hence what value of B to assign to its position. The calibration selected was the one which brought the peaks of the impurity series closest to their expected positions. A correction was made for the change in gain with temperature of the Hall probe of a few per cent. This was measured by cooling the Hall probe in the constant field of a superconducting magnet in persistent mode, figure 10.

Between 65 and 75 Kelvin there was a rapid change from the impurity series to normal magnetophonon oscillations. At intermediate temperatures a single set of peaks appear at intermediate positions rather than both sets of peaks being resolved. This is expected if the peaks in the density of states are greatly broadened by scattering.

With smaller electric fields at low temperatures jagged, non-periodic structure was seen in the magnetoresistance instead of oscillations. The amplitude of this increased as the temperature was reduced. This may be associated with changes in the degree of impact ionisation of the donors, but it could not be demonstrated to be the same from run to run as would be expected if the experimental conditions were perfectly controlled.

B257 devices, which had a similar carrier concentration, also showed this jagged structure at low fields and temperatures. At high fields the magnetoresistance curve became very smooth, showing neither oscillations nor any jagged structure. The reason for this difference is not known, but it may be related to the higher degrees of compensation in the MV73 devices.

Magneto - Phonon Oscillations in Narrow Channels

As the conducting channel of the MESFET is narrowed, the quantum size effect becomes increasingly important. We investigated the magneto-phonon effect, expecting that when the channel became narrow the position of the resonance would shift due to the movement of the Landau levels induced by the electric confirement. Unfortunately, as the channel decreased in width, so the mobility decreased, so this resulted in a disappearance of the oscillations before the shift could be observed.

Future Work

Work under way includes the fabrication of ring structures in GaAs for quantization experiments and studies of the valley-valley interaction in Silicon inversion layers.

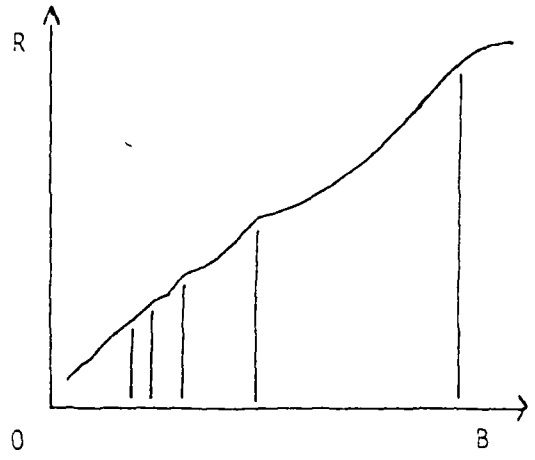

MAGNETOPHONON OSCILLATIONS

FIGURE 1

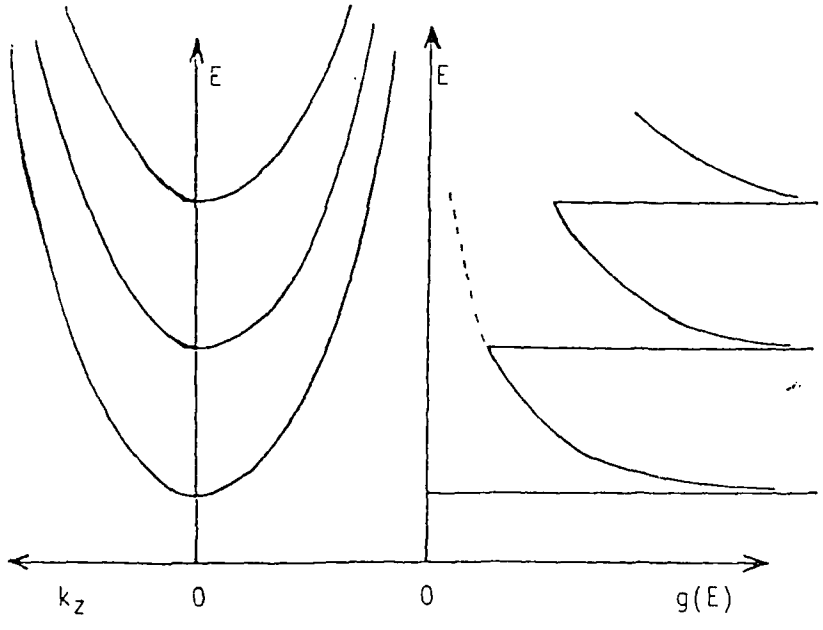

DISPERSION CURVES AND DENSITY OF STATES

FIGURE 2

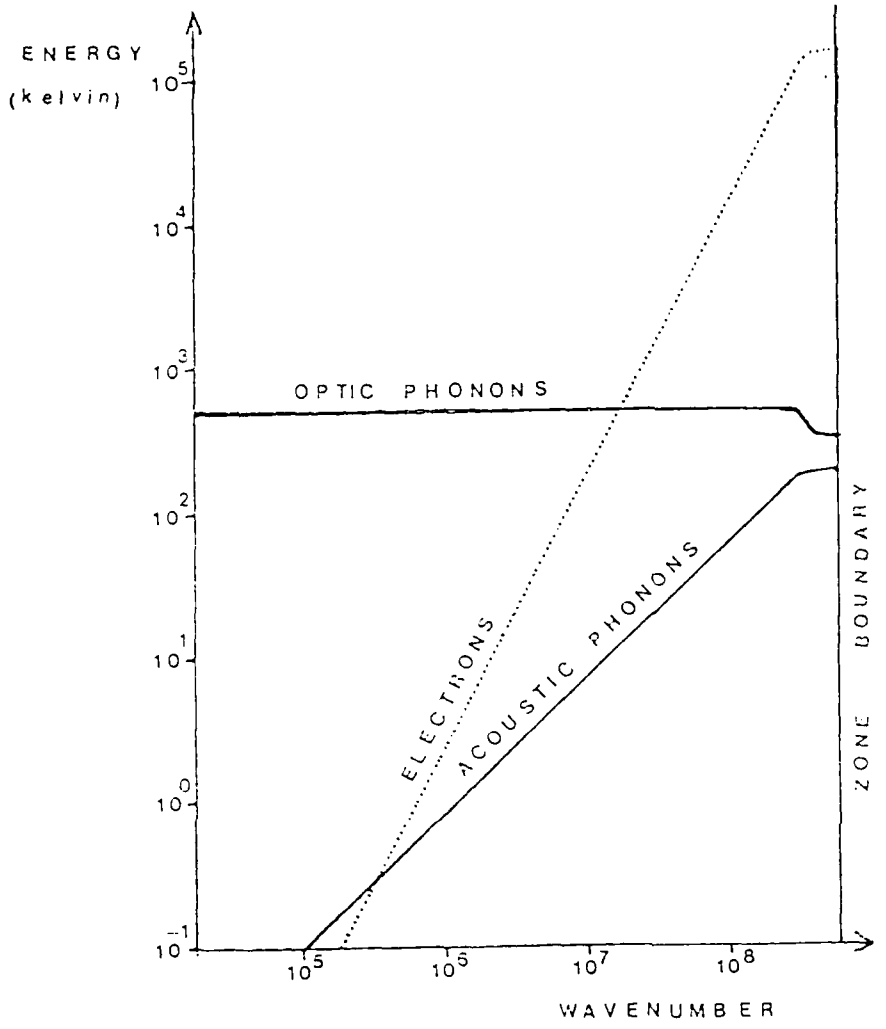
ENERGY
(kelvin)
10^5
10^4
10^3
10^2
10^1
10^0
10^{-1}
OPTIC PHONONS
ELECTRONS
ACOUSTIC PHONONS
ZONE BOUNDARY
10^5
10^6
10^7
10^8
WAVENUMBER

FIGURE 3

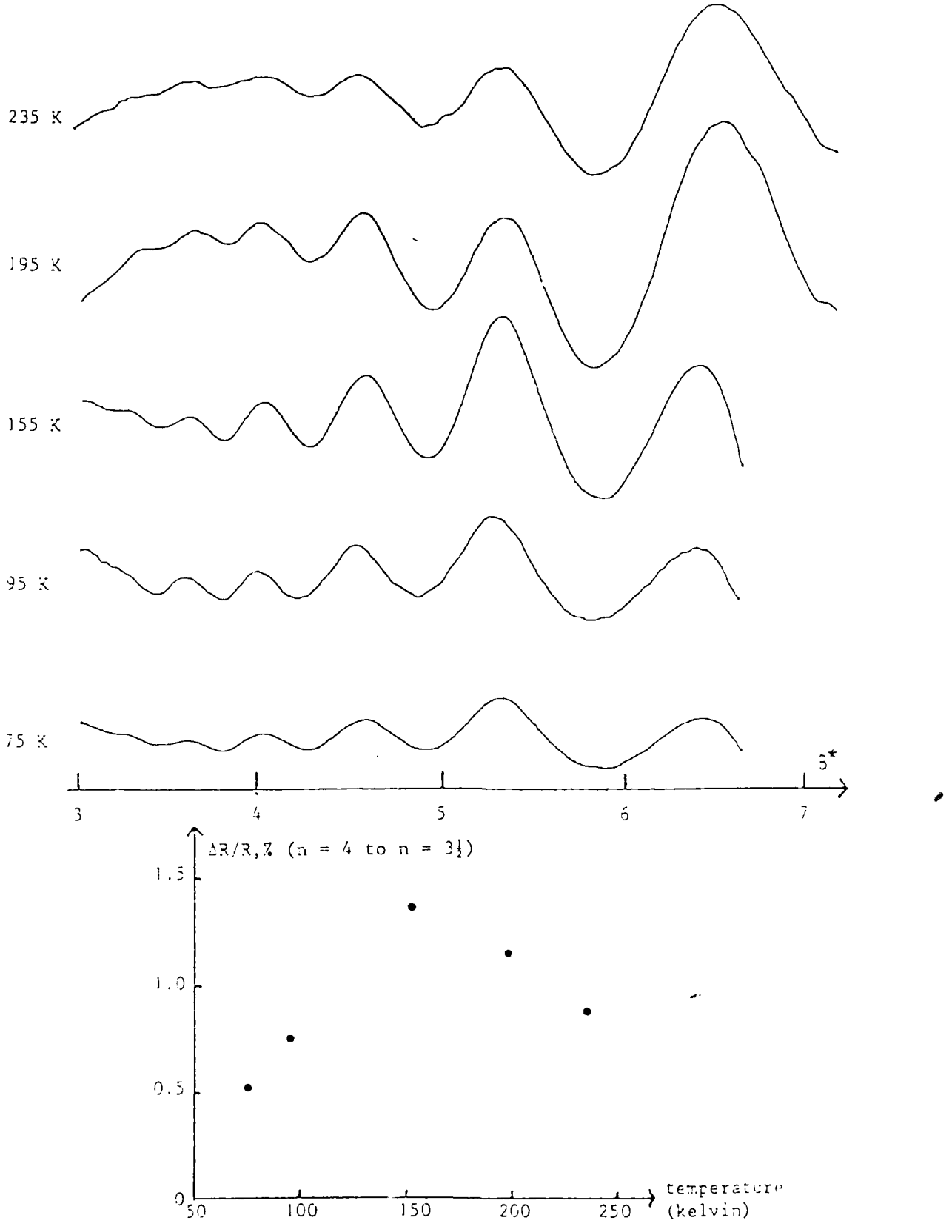
235 K
195 K
155 K
95 K
75 K
δ*
3
4
5
6
7
ΔR/R,% (n = 4 to n = 3½)
1.5
1.0
0.5
0
50
100
150
200
250
temperature
(kelvin)

FIGURE 4

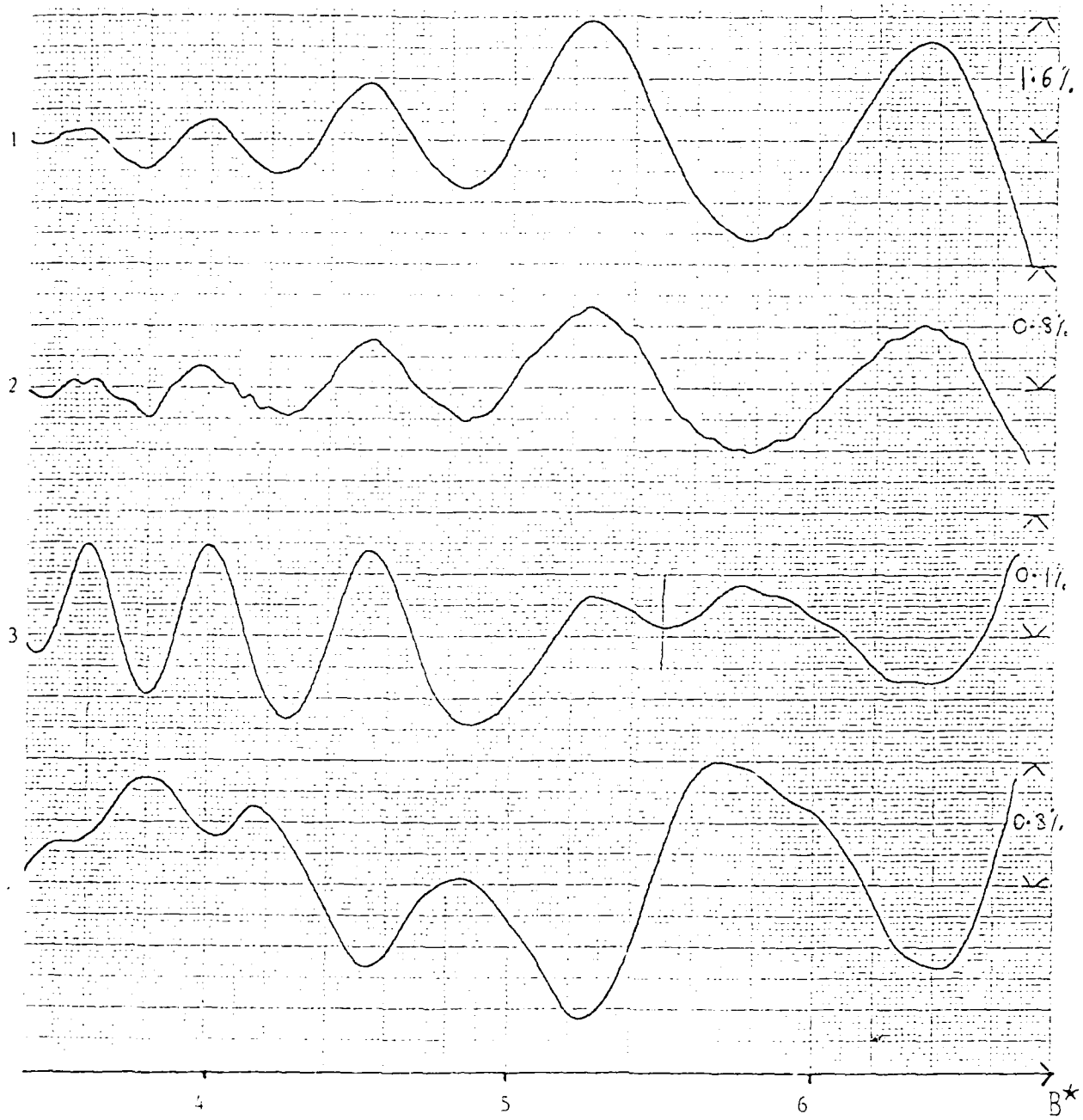

	Aspect Ratio
(1) Long device, B parallel to layer	375
(2) Short device, B parallel to layer	10
(3) Long device, B perpendicular to layer	7
(4) Short device, B perpendicular to layer	0.03

FIGURE 5

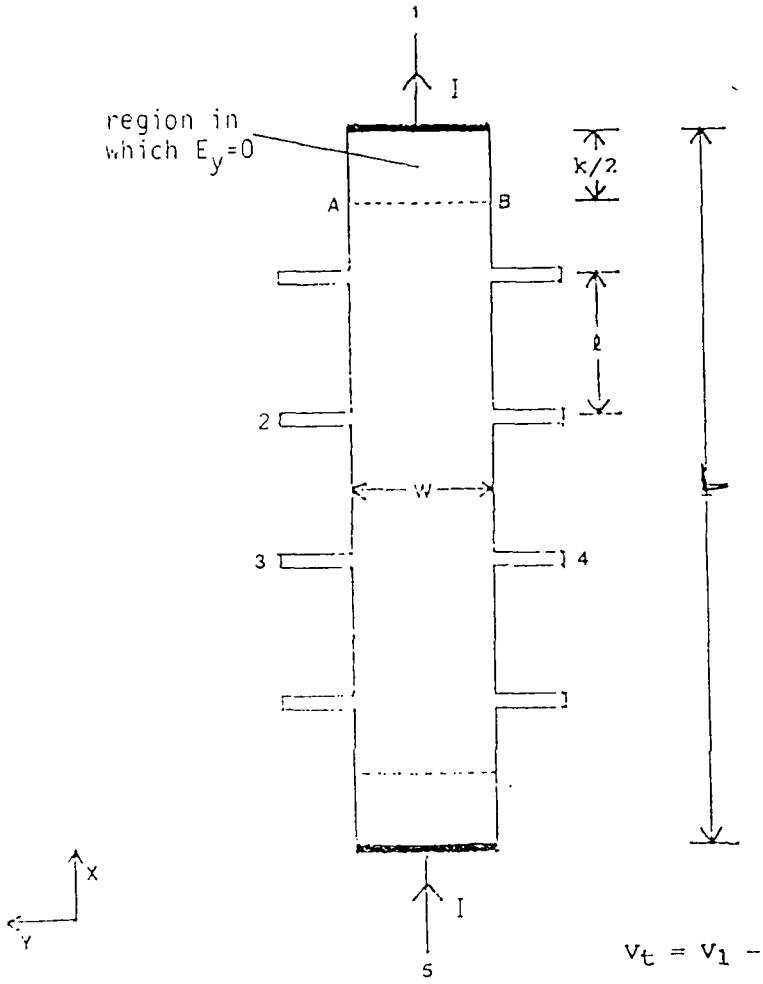

$V_t = V_1 - V_5$

$V_s = V_2 - V_3$

$V_h = V_4 - V_3$

FIGURE 6

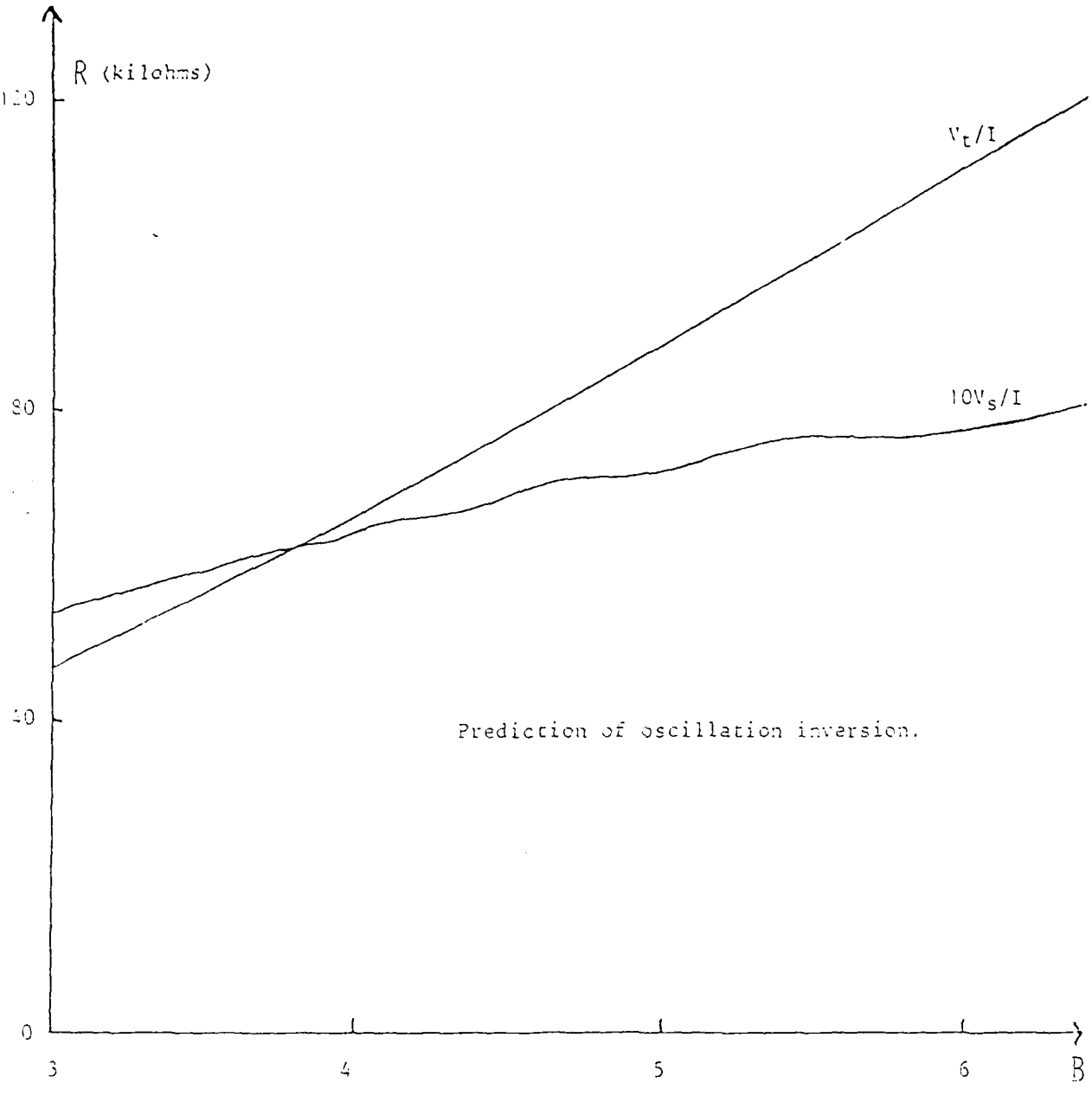

Prediction of oscillation inversion.

FIGURE 7

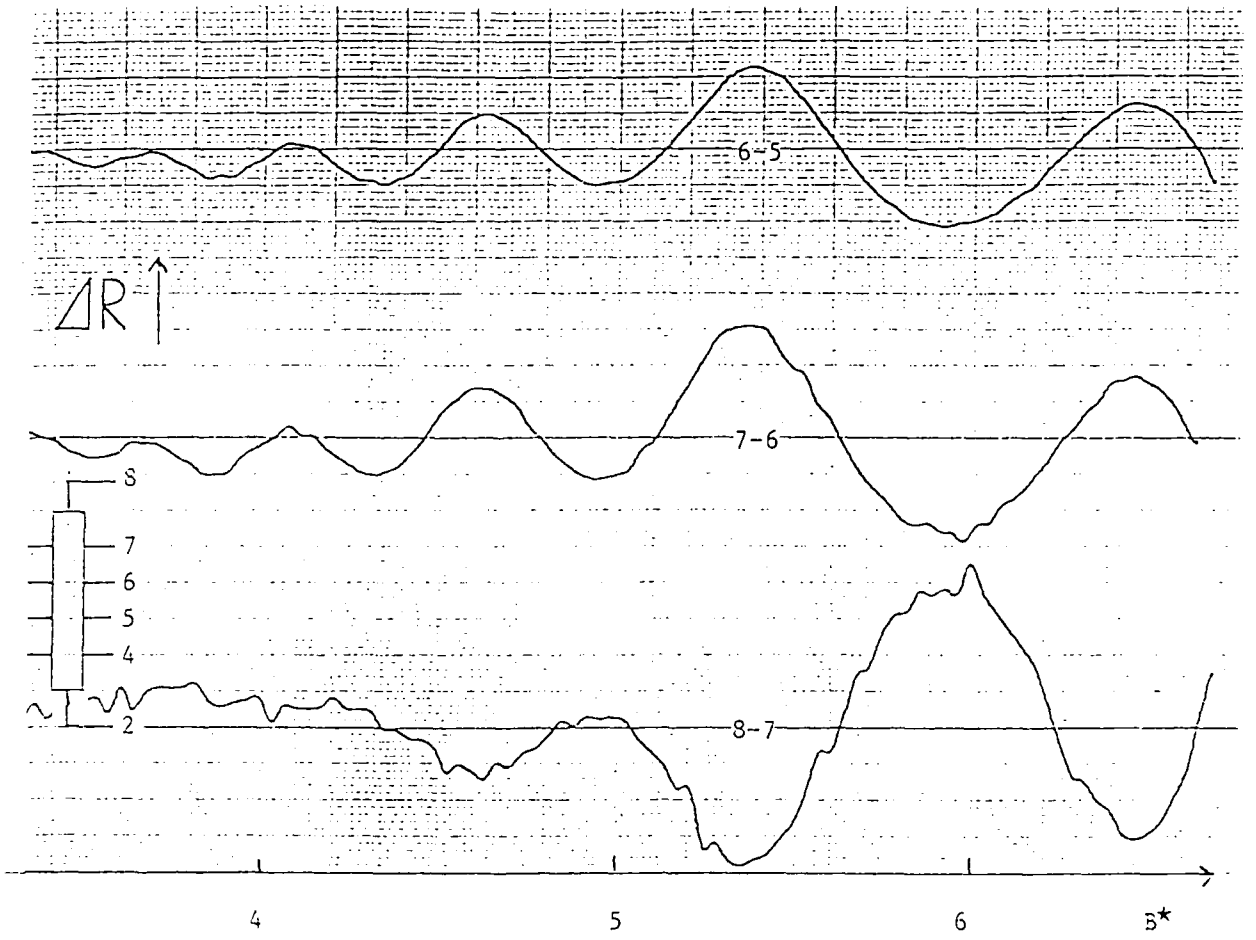

FIGURE 8

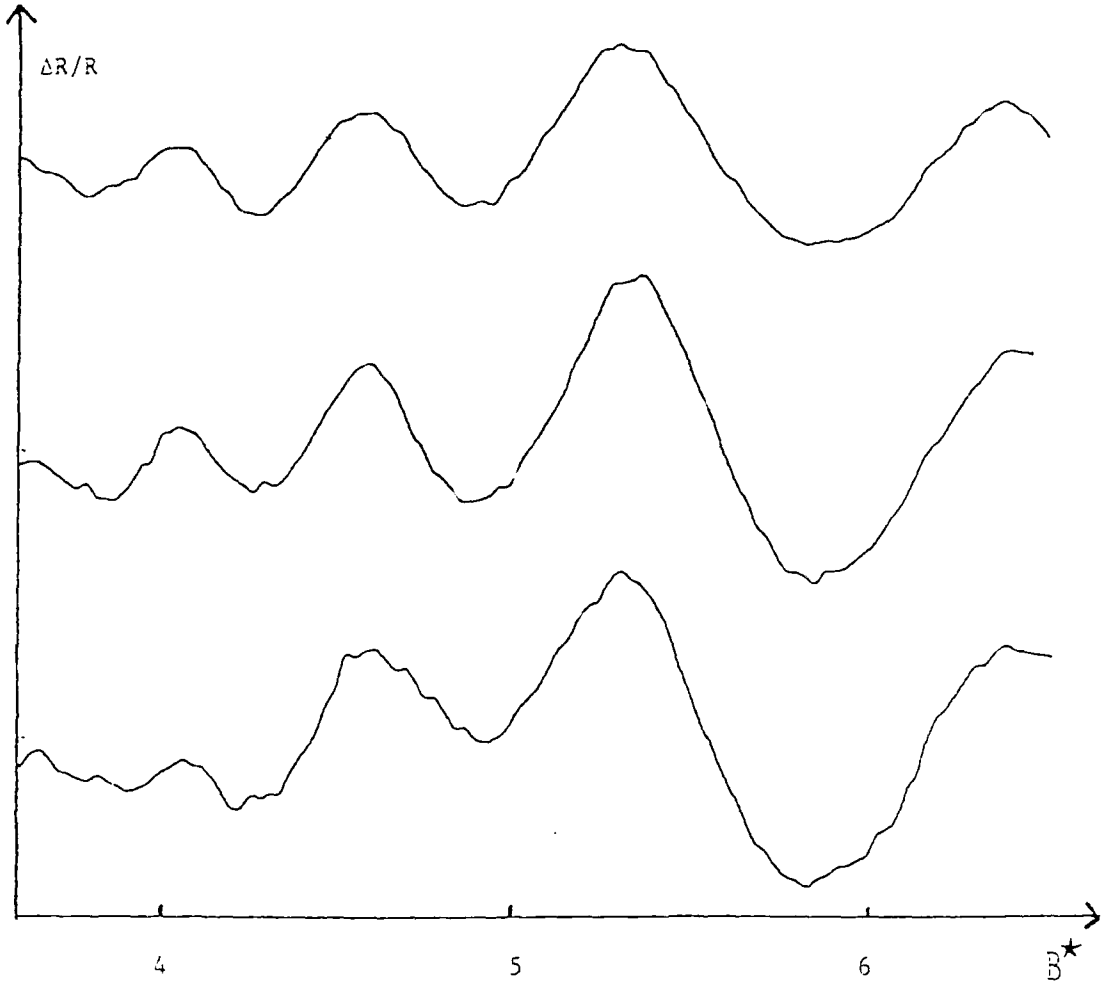

Initial increase in oscillation amplitude in B257 short device.
Traces are for 100, 50 and 25 per cent of zero gate voltage conductance.
Vertical scale: 2cm corresponds to ΔR/R is 0.8%.

FIGURE 9

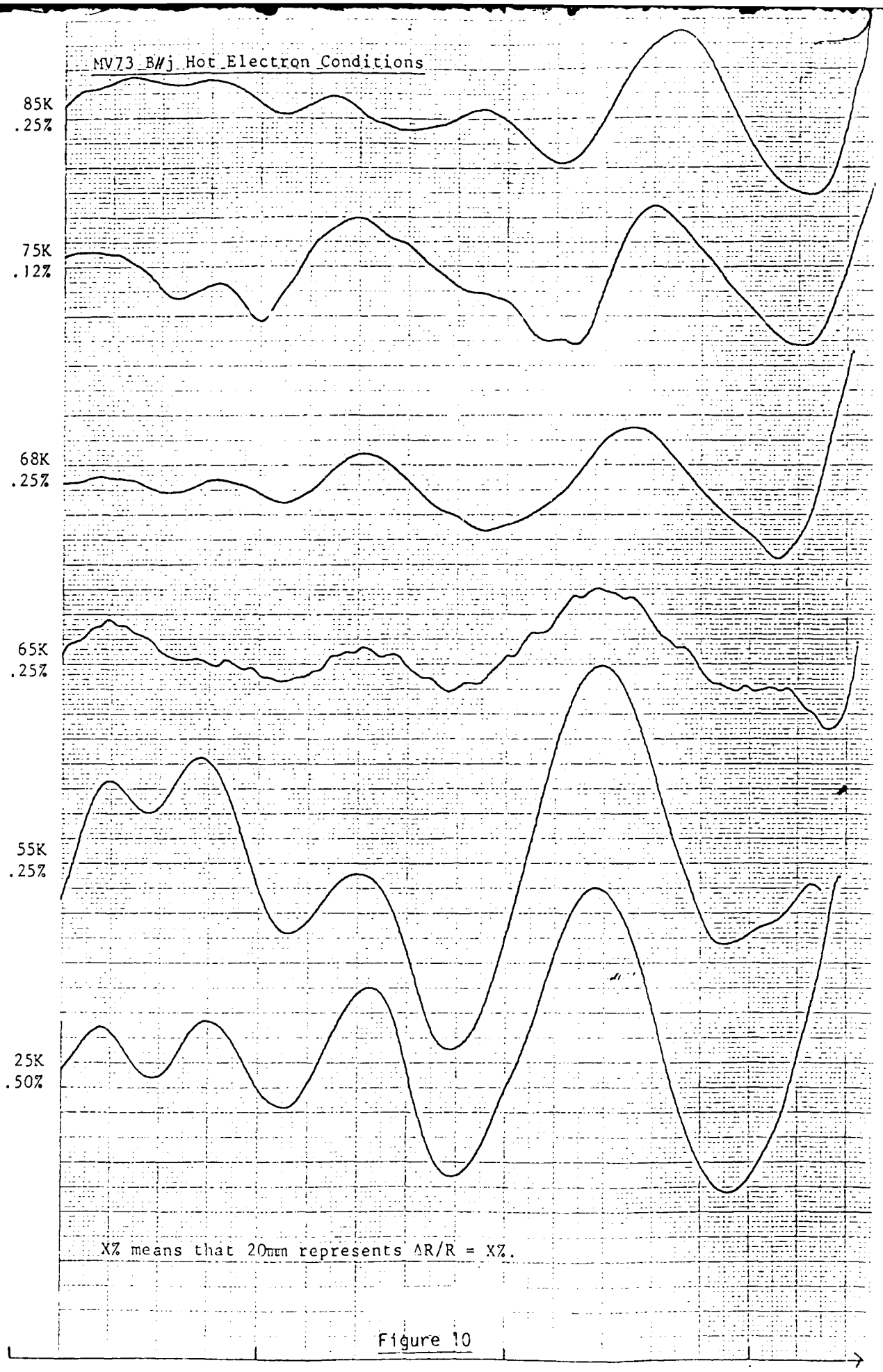
MV73 B#j Hot Electron Conditions
85K
.25%
75K
.12%
68K
.25%
65K
.25%
55K
.25%
25K
.50%
X% means that 20mm represents ΔR/R = X%.

Figure 10

Quantum Phenomena in Semiconductor Structures

Professor M Pepper
Cavendish Laboratory
University of Cambridge
Madingley Road
Cambridge CB3 OHE

Contract: DAJA-85-C-0045
Fifth Interim Report
April 1987 - October 1987

The research reported in this document has been made possible through the support and sponsorship of the US Government through its European Research Office of the US Army.

In this report, we present further results of our investigation into Quantum Phenomena in Semiconductor Structures. The report presents results in three areas,

a) Quantum coherence in GaAs structures.

b) Valley-Valley interactions in Si inversion layers.

c) A novel method for the determination of the electronic specific heat of a semiconductor.

1. Quantum Coherence in GaAs Structures

1.1 Introduction

Quantum-mechanical properties such as the wavelike nature of electrons can be studied in a relatively direct way in devices where the wavefunction is split up and recombines to give rise to quantum interference effects. Loops of a high quality conducting material are suitable for this work, provided that they are small enough and that the temperature is low enough, so that electrons traversing the ring do not suffer inelastic collisions. The resistance of the loop is affected by the interference, and this can be observed by changing the magnetic field through the loop, which changes the phase of the wavefunction, due to the Aharonov-Bohm effect. The magnetoresistance should show oscillations of period h/e as the flux through the ring is varied.

A novel technique has been used to make micron-sized loops of two-dimensional electron gas (2DEG) in GaAs- AlGaAs heterojunctions. A Hall bar device is made using optical lithography, using a set of masks designed for the purpose. The chip is then spin-coated with PMMA electron beam resist, which is then patterned using electron beam lithography. Resist is required to be left in place only over the parts of the ring which are to conduct, so the other regions are exposed with the electron beam and developed away using a standard developer. The whole of the centre of the device is then coated with a thick layer of gold (0.3μm) in such a way as to ensure that the gold rises up the walls of the resist. The regions of gold which touch the surface of the material form gates, which deplete the 2DEG beneath them when they are biased negatively, and further restrict the 2DEG with increasing bias. These gates restrict the 2DEG to narrow regions between them, which are arranged in the form of an annulus with contacts on opposite sides of the ring and adjacent voltage probes for making four-terminal measurements. Increasing the bias on the gates squeezes the conducting channels, allowing width-dependent effects to be studied.

1.2 Results

Ring structures were made using heterojunction material in which the electron mobility varied between 250,000 and 1,000,000 $cm^2/v.s$ at 4.2K. The magnetoresistance of each device was measured in a dilution refrigerator at temperature down to below 100 mK, and magnetic fields up to

13.6T. A range of gate voltages, corresponding to a range of channel widths between 1000Å and 2000 Å, was studied, especially at fairly low fields (<1T), in order to determine the dependence of the Aharonov-Bohm (AB) effect on channel width and field. The Quantum Hall Effect was studied at higher fields.

All the measurement were made at temperatures T<100mK. For mobilities about 500,000 $cm^2/v.s$, the AB effect shows up very clearly as the channel is narrowed. The oscillations are not as readily observable close to zero field as they are at slightly higher field. They then persist up to fields around IT. At various places in this range of field, the oscillations become very much attenuated, probably due to "beating" with Universal Conductance Fluctuations (UCFs), which also show up as random features of amplitude a few times greater than that of the AB oscillations, and characteristic period at least a few times more than the AB h/e period. Towards B = IT, the oscillations die out for longer intervals, and they hardly appear at all above this field. The positions where beating occurs vary with gate voltage, but it is not clear whether the maximum field where the oscillations can be said to have nearly died away varies with gate voltage or not, due to the difficulty in defining this position since it is confused by the beating effect.

As the gate voltage is increased (negatively), the AB oscillations and the UCFs both increase in amplitude out of proportion to the increase in resistance arising from the narrowing of the channel. The maximum amplitude of the oscillations for each device is between 3 and 10% of the total resistance. The device which show the oscillations more clearly are those with highest mobility, and hence, probably, the greatest inelastic scattering length.

The temperature dependence of the oscillations was measured using devices with mobility in the region of 10^6 $cm^2/V.S$, between 800 mK and <100 mK. The oscillations are reduced in amplitude as T increases, and become almost submerged in noise and fluctuations for T≥250-300 mK.

The Quantum Hall Effect (QHE) was seen for field above ~ IT on both types of material. For low gate voltages (at which the device is defined, since the 2DEG is fully depleted underneath the gates, but where the depletion regions have not spread sideways to squeeze the 2DEG channels), the QHE behaves as expected for a 2D device, for both the Hall voltage and the resistance R_{xx}. However, as the gate voltage is increased, the zeroes in R_{xx} at the lowest filling factors (2 or 3), becomes less pronounced, and plateaux start to form, with values of h/e^2j where j is a small integer. This result is unexpected, and it is not yet clear whether it is due to the presence of a loop, or to the fact that the channel is becoming 1D. Further work will be carried out to determine this. The carrier concentration is also found to decrease with increasing gate bias by up to ~30% in the range of gate voltages studied, and this is thought to be a property of split-gate devices in general.

1.3 Conclusion

The use of a split-gate technique to define loops of 2DEG in high-mobility heterojunctions has been shown to produce very good results and to allow the investigation of width-dependent effects which cannot be studied by other techniques at all easily. The potential for use in other types of devices remains yet to be explored.

2. Valley-Valley interactions in Silicon Inversion Layers

2.1 Introduction

In this work, we have studied the role of applied compression on 2D transport in Silicon inversion layers. On the (100) surface, the application of a gate voltage quantizes the inversion or accumulation layer into two sets of subbands. The ground state of the two-fold degenerate light-mass valleys, E_0, is typically 10 meV below that of the four-fold degenerate heavy-mass subband. Application of an uniaxial stress along one of the principal axes in the plane of the channel reduces the energy of the two heavy-mass valleys on the axis and increases that of the other four. Hence an electron transfer into the pair of heavy-mass valleys can be expected and is observed through changes in transport phenomena such as conductivity, mobility and effective mass.

The results obtained can be separated into three sections: 1) results in low magnetic fields, 2) results in high magnetic fields and 3) results on very narrow devices where intrinsic stresses can be expected to be predominant.

2.2 Results in Low Magnetic Fields

Both Hall voltage and magnetorestance data have been obtained in this regime for (100) devices under the influence of uniaxial stress. The data suggests that the electrons, despite undergoing a gradual valley transfer, behave as if they were one carrrier type in a single system. The Hall coefficient, R_H, stays constant even when both the light mass and heavy mass voltages are occupied. In effect, $R_H = 1/ne$ seems to hold rather than

$$R_H = \frac{n_1\mu_1^2 + n_2\mu_2^2}{e(n_1\mu_1 + n_2\mu_2)^2}$$

the equation for conduction in two different subbands. Magnetoresistance data, analyzed on the

basis of the theory for weak localization gives a prefactor $n_v\alpha$ slowly decreasing from $n_v\alpha = 1$ with increasing stress. For unstressed (100) samples at low temperatures where the intervalley scattering time τ_v, is much less than the inelastic scattering time τ_{in}, Fukuyama has shown α is $1/n_v$ or 0.5 (hence $n_v\alpha = 1$). If $\tau_v >> \tau_{in}$, then the electrons will tend to stay within one valley before being inelastically scattered and the individual contributions of the valleys must be added up giving $n_v\alpha = n_v$. The results obtained under stress give $n_v\alpha = 1$ which suggests that, despite the fact that the light and heavy-mass valleys are separated in k-space, intervalley scattering is strong enough to yield $n_v = 4$ $\alpha = 1/4$ unless a solution based on charge density waves is invoked.

The drop of the prefactor $n_v\alpha$ below one is inconsistent with the presence of interactions in the system. Fukuyama (1985) replaces α by $\alpha = (1 + g_2 - 2_{g4})/n_v$ where

$$g_2 - 2_{g4} = -\frac{F}{2}\frac{1}{1 + \frac{F}{2}\ln\left[\frac{1.143\epsilon_F}{T}\right]}$$

are the coefficients for Cooperon orbital interaction induced magnetoresistance in perpendicular magnetic fields.

2.3 Results in High Magnetic Fields

The application of stress on devices under high magnetic field has also been studied. The initial application of stress enhances valley splitting as has been theoretically predicted. The reduction of the transverse conductivity peaks at low stresses can be accounted for by presuming the presence of long band tails of the heavy-mass subband down to the light-mass energy levels. The movement of light mass peaks to high electron concentrations can readily be followed, for the first time, with increasing stress. It is not clear, however, if the observed merging of the peaks and the enhancement of σ_{xx} at concentrations where both the Landau level subbands are occupied can be explained in terms of a simple superposition of peaks from the the heavy and light mass subbands, along with the screening of disorder by energetically-lowered heavy-mass Landau levels or if a more subtle interaction between the two subbands would be a more accurate description. Work in tilted magnetic fields would be highly desirable to clarify this issue. At high stresses, the emergence of the first resolved heavy-mass peak is clearly seen as well as the begining of Landau

level overlap due to a general decrease in the mobility of electrons in the stressed system.

2.4 Results for Narrow Devices

Preexisting internal strains are not usually important when considering the transport of fairly large Si MOSFETS. Calculations and theory suggests that large stresses, which are expected to fall off very quickly with distance, are generated only at the edges of Si-SiO_2 interfaces. The high field and low field behaviour of a narrow device (0.6μm by 180μm) was studied and results suggest that a large compressive intrinsic stress exists within the channel perpendicular to the device. A model was developed to explain the anomalous device behaviour as a compressive stress was applied along the length of the channel. The computation of energy shifts due to applied and intrinsic stresses based on this model accounted well for the data obtained and the presence of a preexisting strain due to the growth of the SiO_2 layer. This has important consequences from the technological point of view as efforts are made to develop smaller and smaller devices.

3. A novel method for the determination of the electronic specific heat of a semiconductor

3.1 Introduction

The purpose of this work was to develop a technique for the measurement of the specific heat of a 2D electron gas. The measurement of the electronic specific heat of a semiconductor system is of interest to anyone considering either the behaviour of electrons in semiconductors or of improvements in the understanding of their theory. It is currently measured by inputting power to the sample and noting the change in temperature that occurs in a nearby bolometer. This change contains contributions from both the electons and the lattice and they are separated by assuming a form for the lattice component. The sensitivity of the method in Si:P requires an excess carrier concentration (n_c) greater than 10^{24} m^{-3}. In the novel method outlined below, the electronic component is measured directly in samples of n-InSb where n_c is less than 5 10^{20} m^{-3}. These experiments were intended to demonstrate the technique, the results were good and future work will concentrate on 2D systems.

In the method, an electric field pulse (F) is applied to the sample and the electrons are heated from the lattice temperature (T_l) to a higher electron temperature (T_e). (The electron temperature is found from the conductivity and the lattice is thermally anchored in a helium bath). In equilibrium

there is a balance between the power input and the temperature gained as follows:

$$\sigma F^2 \tau = \int_{T_i}^{T_e} C_{el}\, dT$$

Where σ is the conductivity and C_{el} is the electronic heat capacity. τ is an electron-phonon scattering time which characterises the rate at which energy is lost to the lattice. At high temperatures this scattering time is very short, but at helium temperatures the principal mechanism is piezoelectric scattering and for $n_c \sim 10^{20}$ m $^{-3}$ (assuming free electron behaviour) the characteristic times are of order 100 nanoseconds. In order to measure times as short as these high frequency techniques have to be used and the results are measured with a boxcar averager. The application of interaction theory to the electronic behaviour around the metal-insulator transition (MIT) predicts that coulomb interactions will cause a gap to occur to the density of states around E_f so that the value of $N(E_f)$ should decrease as the MIT is approached.

3.2 Results

Four samples with electron concentrations close to the MIT have been investigated - three of the samples are on the metallic side and one on the insulating side.

The results obtained for the three metallic samples are shown on graphs 1 and 2. Graph 1 shows the variations of the relaxation time with lattice temperature. Previous work found that the scattering decreases as the temperature is raised or as the electron concentration is increased. Our results show a variation with Temperature, but not as large as predicted - they change by ~ 20% in the range of 1.3 - 4.2 Kelvin, compared with a prediction of ~80%.

Graph 2 shows the heat capacities v. Temperature. These tend to zero with T and are linear. Other workers found that the heat capacity in a degenerate semiconductor decreased to zero at finite temperature - our results disagree with this and are in agreement with the free electron model. However the electronic specific heats, which are given by the slopes of graph 2, are not as large as predicted and the discrepancy between that calculated with the free electron density of states and that found experimentally increases as the MIT is approached. This is in agreement with the interaction theory, and the low density of states is found on both sides of the transition.
Another way of approaching the MIT is to apply a magnetic field to a metallic sample. This has also been investigated although the results in this case are much more ambiguous. It is found that the risetimes decrease as approximately $1/\sqrt{B}$ so that the scattering rate increases as the electrons become more localised. However, this may also be due to the magnetic field reducing the heating effect of the electric field and so the value of the electron temperature. This was also investigated

and it was found that the temperature dependence of the conductivity, which is used to measure the electron temperature ceases to be sufficiently accurate in the region of interest.

Conclusion

The method has been found to allow measurement of the specific heat. It can now be applied to the study of 2D systems such as GaAs - AlGaAs heterojunctions or Si inversion layers.

Future Work

Further experiments on quantum coherence in GaAs structures are being performed and they will be described in the next report. Results will also be presented on valley interactions in Si inversion layers and one dimensional effects in GaAs heterojunctions as well as the Quantum Hall Effect in narrow channels.

Figure 1

Electron – phonon relaxation times v T_l

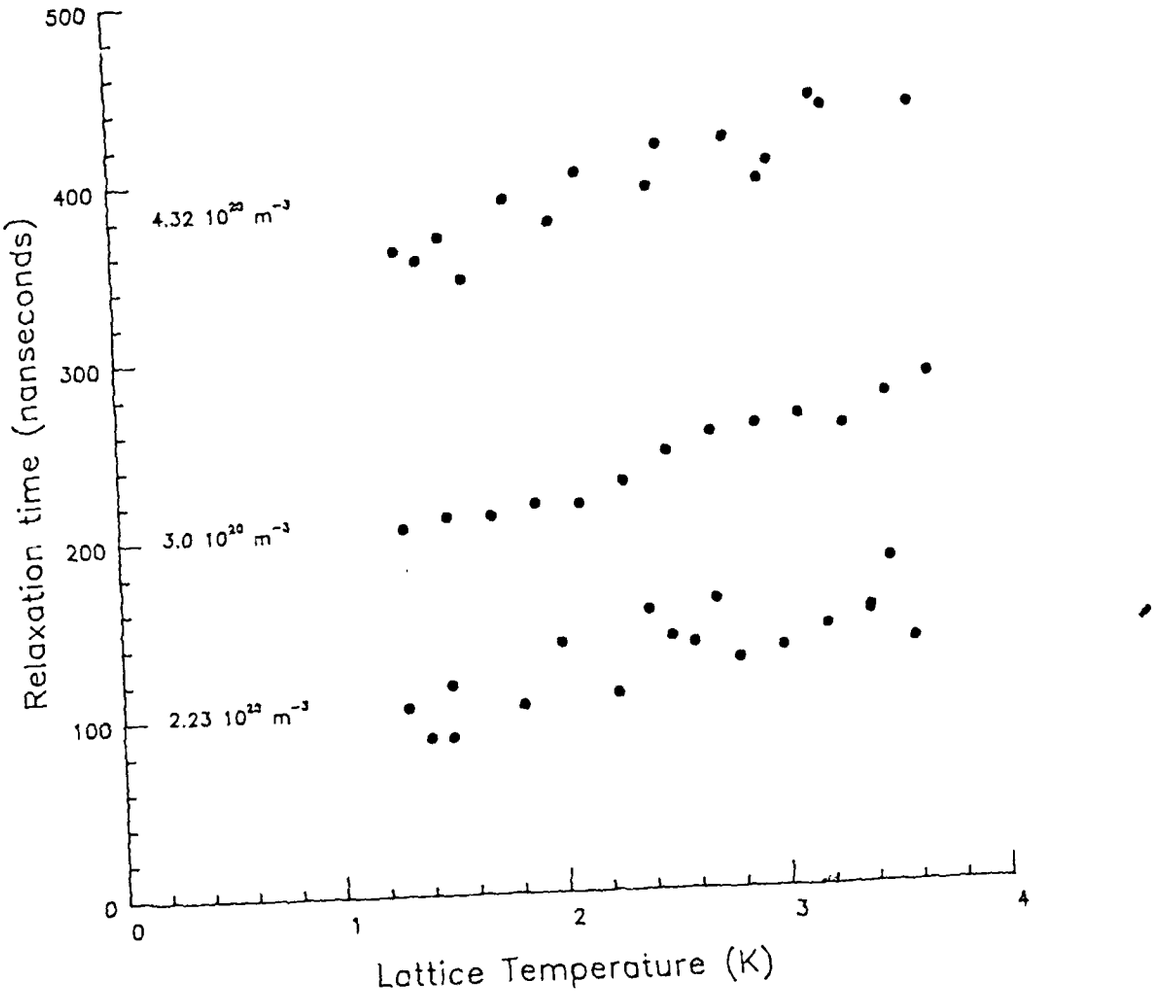

Figure 2

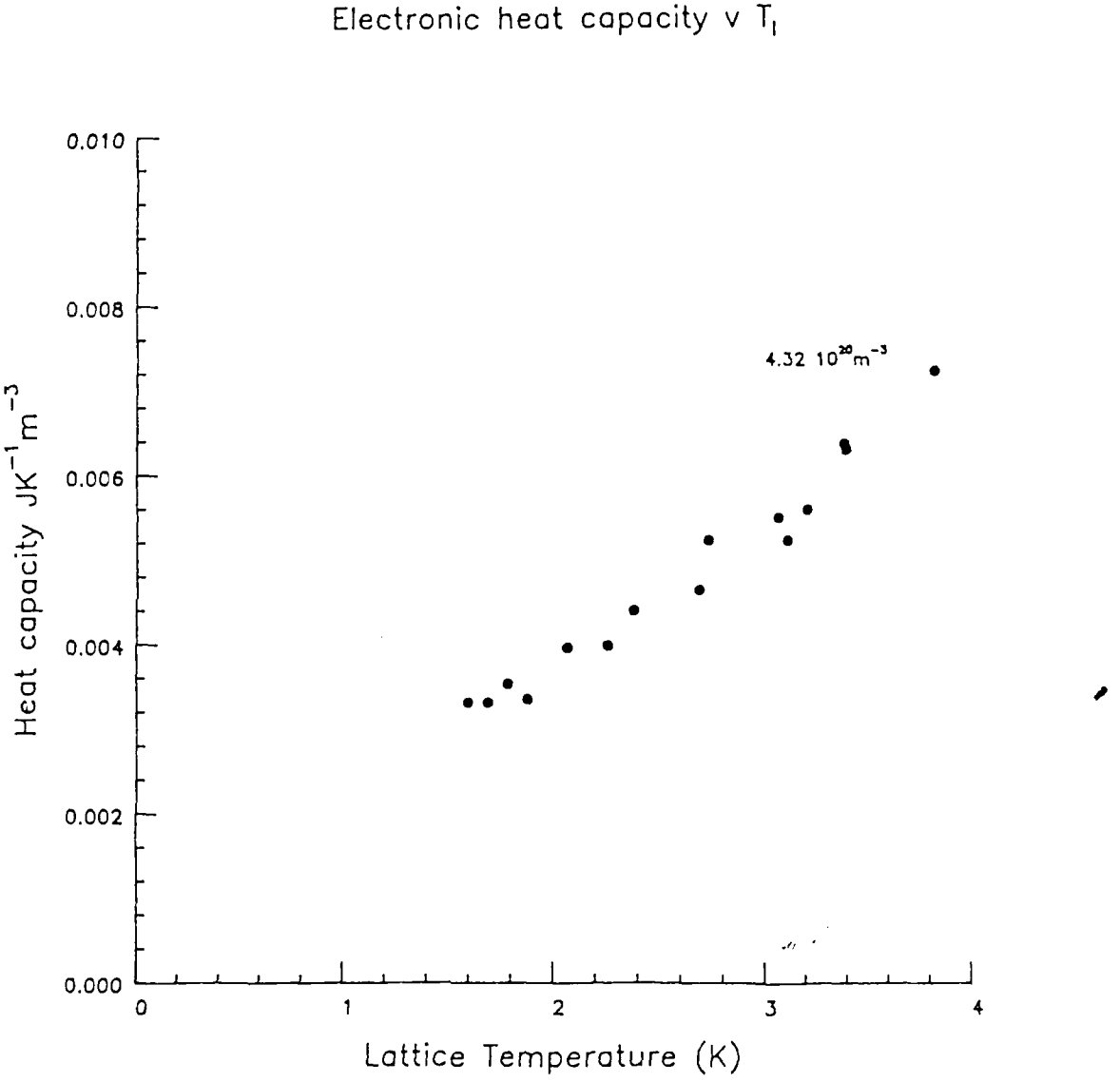
Electronic heat capacity v T_l
0.010
0.008
0.006
0.004
0.002
0.000
Heat capacity $JK^{-1}m^{-3}$
4.32 $10^{28}m^{-3}$
0
1
2
3
4
Lattice Temperature (K)

Quantum Phenomena in Semiconductor Structures

Professor M Pepper
Cavendish Laboratory
University of Cambridge
Madingley Road
Cambridge CB3 OHE

Contract: DAJA-85-C-0045
Sixth Interim Report
October 1987 - April 1988

The research reported in this document has been made possible through the support and sponsorship of the US Government through its European Research Office of the US Army.

1. Introduction

This report consists of the abstracts of 4 papers which have been submitted to Journals. The topics discussed are:

(1) The magnetophonon effect in GaAs Schottky gate FET's in which it is shown that the phase and magnitude of the oscillations are determined by geometrical considerations.

(2) Three papers on the effects of stress on changing the band structure of Si inversion layers with a consequent change of electronic transport properties.

In addition, a reprint is attached of work on quantum coherence in Gallium Arsenide Rings.

2. Present Work

We are investigating the Quantum Hall Effect in narrow channels. Here, the effects on the quantisation of the loss of dimensionality are significant. Further work is being performed on the role of quantum coherence on transport in GaAs rings and ballistic structures. In particular, we are actively considering structures smaller than phase coherence lengths which will allow an addition of different quantum effects.

3. Conclusion

The conclusion of this aspect of our work is that the transport properties of small structures differ radically from larger samples. The wave nature of the electron must be considered when the sample is small and fluctuations arising from small numbers of electrons or impurities must be considered.

The Magnetophonon Effect in GaAs Schottky Gate Field Effect Transistors

T P C Judd and M Pepper

Cavendish Laboratory, University of Cambridge, Cambridge CB3 OHE, UK

and

G Hill

Department of Electrical Engineering, The University of Sheffield, Mappin St,

Sheffield S10 2TN, UK

Abstract

We have investigated the magnetophonon resonance in lightly doped GaAs Schottky Gate Field Effect Transistors of different shape. It is shown that the phase and amplitude of the observed oscillations is dependent upon geometrical considerations, a model is presented in good agreement with experiment.

Electron Magnetotransport in Uniaxially Stressed Si (100) Inversion Layers

N Paquin and M Pepper

Cavendish Laboratory, Madingley Road, Cambridge CB3 OHE, U. K.

A Gundlach and A Ruthven

Edinburgh Microfabrication Facility, King's Buildings, Edinburgh EH9 3JL, U.K.

Abstract

The transverse conductivity, σ_{xx}, of uniaxially stressed Si(100) inversion layers has been measured at low temperatures. The initial application of uniaxial stress leads to an increase in valley-splitting and a reduction of conductivity maxima. Conductivity peak movements at intermediate stresses suggest the presence of valley-coupling or a subband-subband electron exchange interaction. A strong increase of light-mass subband conductivity was also observed and is attributed to heavy-mass subband occupation. There is also evidence for valley-splitting in the heavy-mass subband.

Negative Magnetoresistance in Uniaxially Stressed Si(100) Inversion Layers

N Paquin and M Pepper

Cavendish Laboratory, Madingley Road, Cambridge CB3 OHE, U. K.

A Gundlach and A Ruthven

Edinburgh Microfabrication Facility, King's Buildings, Edinburgh EH9 3JL, U.K.

Abstract

We have studied the negative magnetoresistance of a two-dimensional electron gas in uniaxially stressed Si(100) MOS transistors. The decrease in the fitting parameter α, which is qualitatively explained on the basis of electron-electron interactions, suggests the presence of strong intervalley scattering between heavy- and light-mass subbands. The temperature dependence of τ_{in} supports the modification of the Landau-Baber scattering term in the presence of significant disorder.

Intrinsic Stress in Narrow Silicon MOS Field Effect Transistors: Magnetotransport Measurements

N Paquin and M Pepper

Cavendish Laboratory, Madingley Road, Cambridge CB3 OHE, UK

A Gundlach and A Ruthven

Edinburgh Microfabrication Facility, King's Buildings, Edinburgh EH9 3JL, UK

Abstract

Measurements of the Hall (ρ_{xy}) and transverse (ρ_{xx}) resistivities in narrow polysilicon-gated Si(100) field-effect transistors have been obtained. The measurements were carried out both with and without externally applied uniaxial stress. Analysis of the results suggests the presence of large compressive intrinsic edge stresses. A model based on device fabrication is developed to explain the presence of these edge stresses.

J. Phys. C: Solid State Phys. 21 (1988) L325–L331. Printed in the UK

LETTER TO THE EDITOR

The Aharonov–Bohm effect in electrostatically defined heterojunction rings

C J B Ford†, T J Thornton†, R Newbury†, M Pepper†, H Ahmed†, C T Foxon‡, J J Harris‡ and C Roberts‡

† Cavendish Laboratory, Cambridge CB3 0HE, UK

‡ Philips Research Laboratories, Redhill, Surrey RH1 5HA, UK

Received 3 February 1988

Abstract. Micrometer-sized loops of two-dimensional electron gas have been made on GaAs–AlGaAs heterostructures by electrostatic confinement. A split gate is used to define the loop, allowing the width of the conducting channels to be varied by changing the gate voltage. The magnetoresistance has been measured at low temperatures ($T < 100$ mK) and shows strong Aharonov–Bohm oscillations with amplitudes of up to 7% of the total resistance in the narrowest devices. The oscillations are strong out to $B \simeq 0.5$ T and then die out as B increases to $\simeq 1$ T, with a possible dependence on the channel width. Magnetic depopulation of the 1D sub-bands is also seen.

In small ring structures at low temperatures, the wave-like nature of the conduction electrons becomes readily apparent, because of quantum interference between the parts of the electron wavepacket travelling around opposite sides of the ring. An electron wave packet entering through a contact on one side of the loop splits up, and recombines when leaving through another contact on the opposite side or after travelling the whole way around the loop. In the absence of inelastic scattering both parts of the wave packet are coherent and they interfere, changing the resistance of the device. The interference may be observed through the addition of an extra phase difference between the two waves. The Aharonov–Bohm effect gives rise to such a phase change when a magnetic field is applied perpendicular to the loop. This leads to oscillations in resistance which are periodic in the flux through the ring, with period h/e for waves which travel only half-way around the loop before recombining. These oscillations have been studied extensively in normal metal rings, (Sharvin and Sharvin 1981, Pannetier *et al* 1984, Webb *et al* 1985, Washburn and Webb 1986) where the maximum amplitude observed is only 0.1% of the overall resistance, but only very recently have they been seen in rings made from high-mobility GaAs–AlGaAs heterojunctions, where the maximum amplitude seen so far is 5–10% (Timp *et al* 1987; Ford *et al* 1988). In all previous work, the rings have had their geometry fixed by the fabrication process, but since many properties of the device depend on the channel width, it is clearly advantageous to be able to vary this in a given device.

In this Letter we present results from a micrometer-sized heterojunction ring formed using a novel technique involving a split gate on the surface of the material, which allows

0022-3719/88/100325 + 07 $02.50

the width of the conducting channel to be varied by changing the gate voltage. Aharonov–Bohm oscillations of period h/e are seen, and their amplitude increases as the channel is narrowed. The ratio of the amplitude to the total resistance of the device also increases, up to a maximum of ~7%. The oscillations beat with aperiodic fluctuations, and persist up to between 0.5 and 1 T without much attenuation, and then the amplitude starts to decrease and the oscillations become more intermittent, eventually dying out at magnetic fields between 1 and 1.3 T. At higher fields the quantum Hall effect is seen for the wider channels and magnetic depopulation of 1D subbands occurs for the narrower channels.

The devices used in the present work are made from GaAs–AlGaAs heterojunctions in which a very high-mobility two-dimensional electron gas (2DEG) is formed at the interface between the two materials. A Schottky gate can be formed by depositing a layer of gold on the surface, and applying a negative voltage to this gate depletes the 2DEG beneath it. If a gap about 1 μm wide is left in the middle of the gate, a narrow

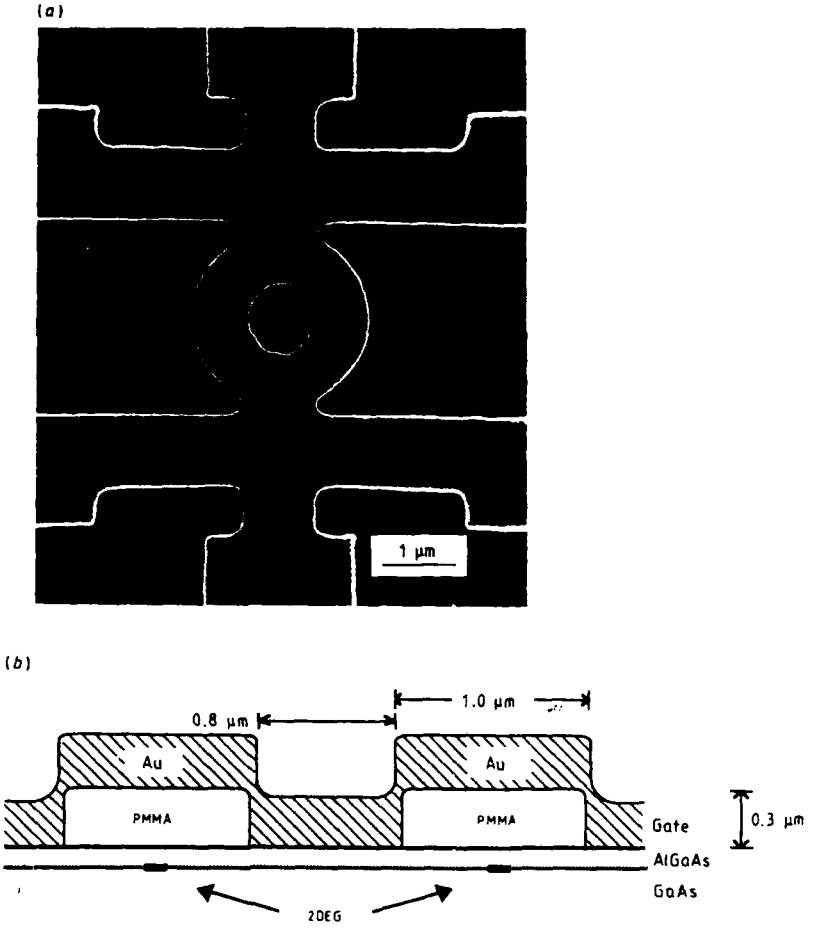

Figure 1. (*a*) An SEM micrograph of an exposed resist loop prior to metallisation: (b) a cross-sectional diagram of the device.

channel of 2D gas remains after the rest has been depleted, and becomes progressively narrower as the gate bias is further increased, until it disappears altogether. In previous work we have used split gates to produce narrow straight devices (Thornton *et al* 1986, Berggren *et al* 1986), and this technique has now been extended to make rings of 2DEG in which the channel width can be varied by changing the gate voltage V_g, down to a minimum width of 150 ± 50 nm.

The gate in the centre of the ring has to be very small (<1 μm) and in order to make contact to it, the whole device is covered in a layer of metal. A spacer layer is used to keep the metal away from the surface of the material in the regions where gaps in the gates are required. The PMMA resist used in the electron beam lithography is the easiest spacer layer to use, since little further processing is required after exposure to the electron beam. Full details of the process are described elsewhere (Ford and Ahmed 1987). Figure 1 shows a picture of the loop and a schematic diagram of its cross section.

A loop was made on a GaAs–AlGaAs heterojunction with a mobility of about $100\ m^2\ V^{-1}\ s^{-1}$ at 4.2 K. The four-terminal magnetoresistance was measured in a dilution refrigerator at temperatures down to <100 mK using standard phase-sensitive techniques. The device was found to become defined when the regions directly beneath the gates became fully depleted, at a gate voltage $V_g = -0.36 \pm 0.01$ V, and it pinched off at $V_g \simeq -2.3$ V. Aharonov–Bohm h/e oscillations are seen as the magnetic field is varied, for a range of gate voltages, as shown in figure 2(a). The oscillations are superimposed upon reproducible, aperiodic fluctuations (Lee and Stone 1985) and become very pronounced as the channel is narrowed by making the gate voltage more negative. They are at most about 7% of the total resistance. The oscillations beat with the fluctuations, so that in places the oscillations almost disappear for a short interval of magnetic field. These intervals are not regularly spaced, showing that the beating is with fluctuations rather than with a second frequency. The fluctuations are also much larger for the narrower channels, but the change in conductance $\Delta g \simeq e^2/h$ for each V_g, as expected.

Figure 2(b) shows the Fourier transforms of some of the results shown in figure 2(a). The peak due to the h/e oscillations is clearly visible, and it gets narrower as the gate voltage is increased. The flux enclosed by an electron trajectory can vary between the values corresponding to the inside and the outside diameters of the channel, and the width of the Fourier peak should reflect this uncertainty in the flux, so the observed reduction in the peak width indicates that the conducting channel itself is narrowed by increasing the gate voltage. The channel widths w_{FT} deduced in this way are shown in table 1. It is evident that they consistently give much smaller values for the width than do the other methods, which will be described below. A weak $h/2e$ peak is present in the data for the narrowest channel, due to the electron wavefunction propagating all the way around the ring before recombining rather than just going half way as happens for the h/e period oscillation. This is not the same $h/2e$ oscillation that occurs in connection with weak localisation, as such oscillations are quenched by magnetic fields greater than a few flux quanta h/e (Al'tshuler *et al* 1981). The ratio of the h/e and $h/2e$ amplitudes is $(9 \pm 2):1$. If the amplitude of the oscillation is assumed to decay as $\exp(-L/L_\varphi)$, where L is the distance travelled by the electron before interfering, and if the contacts are assumed to be only weakly coupled to the ring so that they do not add to the inelastic scattering, then $L_\varphi \geqslant 2.5$ μm.

The oscillations remain on average unattenuated up to fields of between 0.5 and 1 T, depending on gate voltage, and then start to decay and become intermittent, so that when B reaches 1–1.3 T, they have almost died out, except for occasional bursts of activity. It is difficult to determine accurately the field B_{max} at which the oscillations can

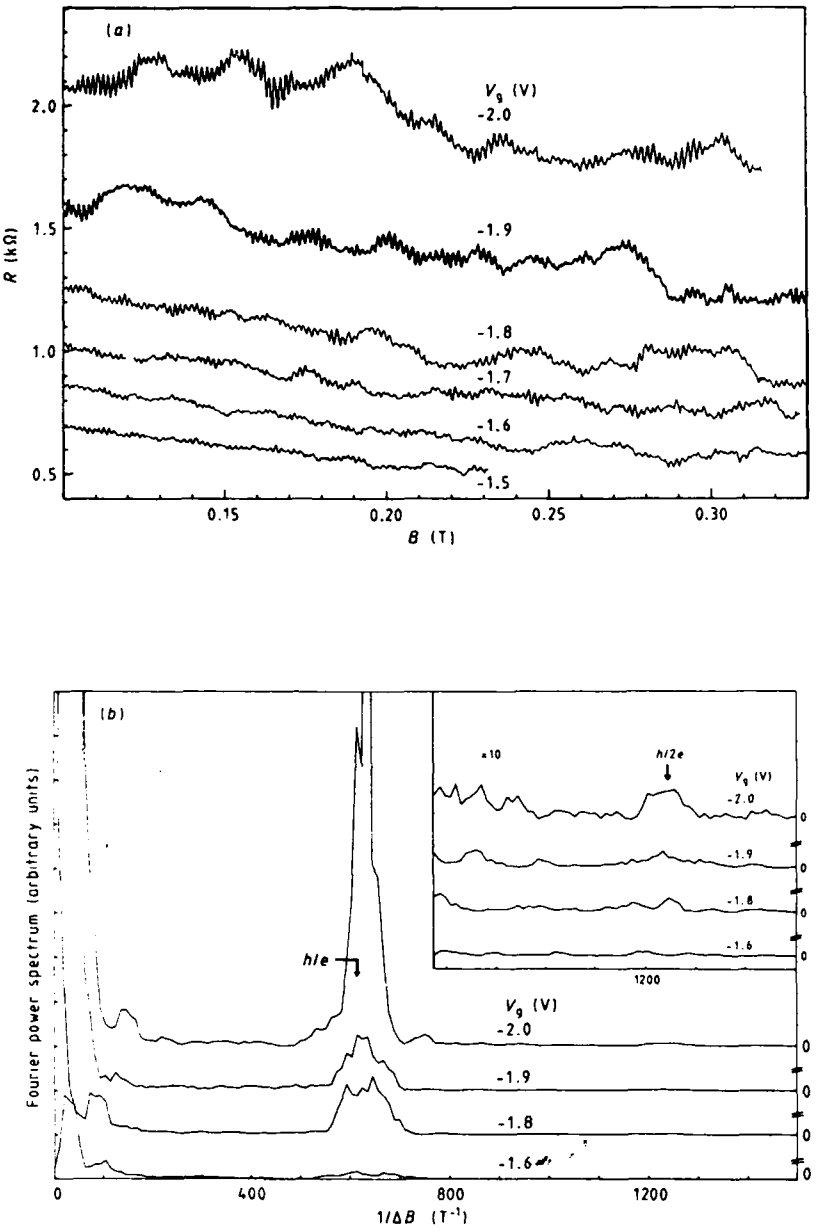

Figure 2. (*a*) The magnetoresistance as a function of the gate voltage (shown in volts by each curve), for $0.1 < B < 0.33$ T. The h/e period is 1.6 mT. (*b*) The Fourier transforms of the data in (*a*) after subtraction of the background negative magnetoresistance. The arrows indicate the position of the h/e period for a loop of radius 0.9 μm, equal to the average of the inner and outer radii of the resist loop. The curves have been offset for clarity. The inset shows the region around 1200 T^{-1} with the vertical axis expanded by a factor of ten, to show the $h/2e$ peak.

Table 1. The channel widths deduced from various methods, as a function of gate voltage V_g; w_{depop} is the width deduced from fitting the theory to the depopulation data shown in figure 3; w_{FT} is the width estimated from the width of the peak in the Fourier transform of the Aharonov–Bohm oscillations; $w_{B_{max}}$ is from the approximate field B_{max} at which the Aharonov–Bohm oscillations appear to die out.

V_g (V)	w_{depop} (μm)	w_{FT} (μm)	$w_{B_{max}}$ (μm)	n_s (m^{-2})
−0.4	(0.95 ± 0.05) nom			3.22 ± 0.03
−1.6	0.36 ± 0.01	0.18 ± 0.02		2.26
−1.91	0.29	0.12 ± 0.02	0.18 ± 0.03	1.8
−2.02	0.24 ± 0.02	0.10 ± 0.02	0.14 ± 0.03	1.6
−2.09	0.18 ± 0.03	0.10 ± 0.02	0.10 ± 0.025	1.4
−2.3	pinches off			

be said to have died out or to have decayed to a certain fraction of the low-field amplitude, but it is possible to estimate it for each gate voltage. It has been suggested (Timp *et al* 1987) that the oscillations should die out when $(\hbar/eB)^{1/2} \simeq w/2$, where w is the width of the channel, due possibly to electrons becoming localised in one arm of the ring and therefore not contributing to the interference. This gives very small widths compared with the values given by other methods. We can take the Landau level index into account, by taking the cyclotron radius $L_c(B) = [\hbar(2n_L + 1)/eB]^{1/2}$, where n_L is the index of the

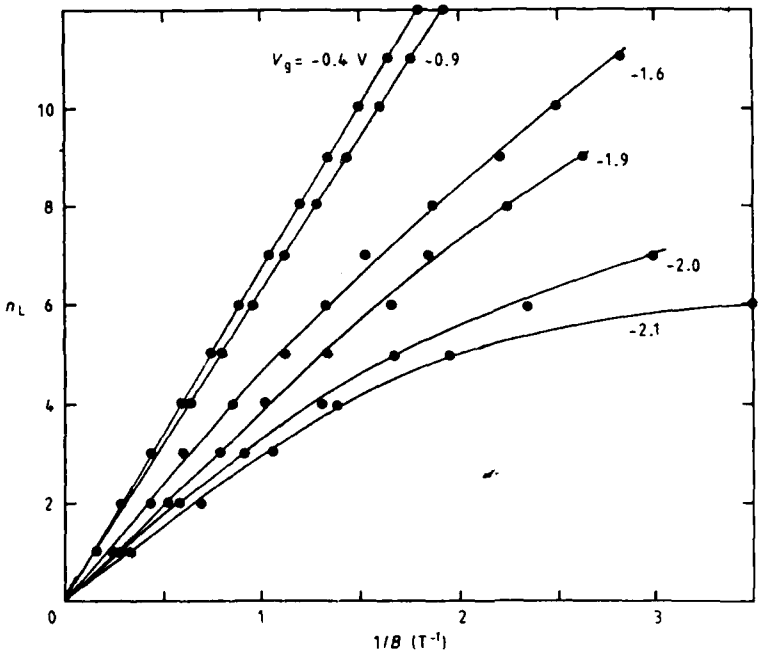

Figure 3. A fan diagram showing the positions of the minima in resistance plotted as a function of inverse magnetic field, for a range of gate voltages. Full curves are only a guide to the eye. The widths deduced from the theoretical fits to this data are given in table 1.

maximum Landau level occupied at $B = B_{max}$, deduced from the Shubnikov–de-Haas data shown below. The values of w calculated from $L_c(B_{max}) \simeq w/2$ are shown in table 1. Although there is not enough data at present to see a trend, the values for the width are more reasonable. The mobility μ of the device when the channel has just been defined, i.e. at $V_g \simeq -0.4$V, is greater than $50\,m^2\,V^{-1}\,s^{-1}$, and is probably around $100\,m^2\,V^{-1}\,s^{-1}$, similar to that of the unpatterned material. As shown in table 1, the carrier concentration n_s decreases as V_g is made more negative, so that $n_s(V_g = -2\,V)$ is about half the value at $V_g \simeq -0.4\,V$. If ionised impurity scattering dominates in this material (Paalanen *et al* 1984), then $\mu \propto n_s^{1.65}$, so $\mu(V_g = -2\,V) \simeq 0.3\mu(V_g = -0.4\,V)$, i.e. $15\,m^2\,V^{-1}\,s^{-1}$ (or $30\,m^2\,V^{-1}\,s^{-1}$ if $\mu \simeq 100\,m^2\,V^{-1}\,s^{-1}$ at $V_g \simeq -0.4\,V$) Thus the oscillations extend to fields where $\omega_c\tau = \mu B \geqslant 15$, τ being calculated from the low-field mobility. The elastic length $l_e[= \mu\hbar(2\pi n_s)^{1/2}/e] \geqslant 1\,\mu m$.

At high magnetic fields, Shubnikov–de-Haas oscillations and the quantum Hall effect are seen, but as the device is narrowed, these become masked by fluctuations, especially at fairly low fields. The quantum Hall plateaus corresponding to filling factors $\nu \geqslant 4$ narrow and disappear. If the Landau level index corresponding to each minimum in resistance is plotted against $1/B$, as shown in figure 3, the lines are not straight as they are for a wide device, but they bend downwards at high values of n_L, and the bending increases as the channel is narrowed. This agrees with the theory of Berggren *et al* (1986, 1988) in which the magnetic depopulation of one-dimensional sub-bands gives rise to oscillations in the magnetoresistance. The sub-bands are formed when the width of the channel is not much greater than the Fermi wavelength. The energy separation of the sub-bands increases in the presence of a perpendicular magnetic field and the magnetoresistance oscillates as the Fermi energy passes through each level in turn. The curves in figure 3 have been fitted to the theory assuming a parabolic potential which gives the result

$$N_e^{1D} = \frac{2}{\pi}\left(\frac{2m^*}{\hbar}\right)^{1/2}\left(\frac{\omega^{3/2}}{\omega_0}\right)\sum_{\nu=1}^{n}\nu^{1/2}$$

where N_e^{1D} is the number of electrons per unit length, ω_0 is the characteristic frequency defining the strength of the confinement, $\omega = (\omega_c^2 + \omega_0^2)^{1/2}$ and n is the index of the sub-band which is just being depopulated. The best fit to each curve yields a value for the width which is fairly insensitive to the exact fitting parameters. Table 1 gives the values together with errors estimated from the spread of values for each curve. The table also shows values for the width deduced from other methods detailed above, for a series of different gate voltages. The widths w_{depop} derived from the magnetic depopulation are consistently larger than those obtained from the Fourier transforms. This may be due to the uncertainty of defining an effective width for a parabolic potential. Also, for widths $\geqslant 0.2\,\mu m$ the potential is unlikely to be parabolic. However, for $V_g = -1.6\,V$, $w_{depop}(\simeq 0.36\,\mu m)$ agrees approximately with the width deduced from the resistance, measured at a field at which the strong negative magnetoresistance has almost disappeared but low enough for Shubnikov–de-Haas oscillations to be of very low amplitude. The widths w_{FT} deduced from the spread of the Fourier transforms of the Aharonov–Bohm oscillations are less than w_{depop} by about a factor of two, and this may be a consequence of the lack of scattering in the loop, and of the specular nature of the scattering from the walls. In such a case, the electrons will probably not sample all the possible paths through the loop, and therefore the range of areas enclosed will be reduced. This contrasts with the case in normal metals, where electrons undergo many

collisions during the passage through the ring, and therefore can be expected to sample the whole area of the conductor, in agreement with experimental results (Washburn *et al* 1985).

In conclusion, a novel technique has been developed to produce rings of quasi-1D high-mobility electron gas in GaAs–AlGaAs heterojunctions, using a split-gate technique. The width of the conducting channels may be varied from 900 down to $\simeq 150 \pm 50$ nm by changing the gate voltage. Aharonov–Bohm oscillations with a maximum amplitude of about 7% of the total resistance of the loop are seen, with a much smaller $h/2e$ component discernible in the narrowest ring. The widths can be estimated from various methods such as magnetic depopulation of the 1D sub-bands, the field at which the Aharonov–Bohm oscillations die out, and the width of the h/e peak in the Fourier transform of the oscillations. The latter gives much smaller values for the width than the other methods.

We thank Professor K-F Berggren for useful discussions about magnetic depopulation, and M Fice for his help in constructing the e-beam lithography machine. One of us (CJBF) acknowledges an SERC studentship. This work has been supported in part by the European Research Office of the US Army.

Note added in proof. Optimisation of ring geometry has established further features of the Aharonov–Bohm effect in electrostatically defined rings. These are the following:

(i) the oscillation amplitude can be as high as 18%;
(ii) AAS ($h/2e$) oscillations have been observed at close to zero magnetic field;
(iii) $h/2e$ and $h/3e$ oscillations are observed at fields higher than for case (ii) above.

References

Al'tshuler B L, Aronov A G and Spivak B Z 1981 *JETP Lett.* **33** 94
Berggren K-F, Roos G and van Houten H 1988 unpublished
Berggren K-F, Thornton T J, Newson D J and Pepper M 1986 *Phys. Rev. Lett.* **57** 1769
Ford C J B, Thornton T J, Newbury R, Ahmed H, Pepper M, Andrews D and Davies G J 1988 *Superlatt. Microstruct.* at press
Ford C J B and Ahmed H 1987 *Proc. Microcircuit Engineering (Paris) 1987* (Amsterdam: North-Holland)
Lee P A and Stone A D 1985 *Phys. Rev. Lett.* **55** 1622
Paalanen M A, Tsui D C, Gossard A C and Hwang J C M 1984 *Phys. Rev.* B **29** 6003
Pannetier B, Chaussy J, Rammal R and Gandit P 1984 *Phys. Rev. Lett.* **53** 718
Sharvin D Yu and Sharvin Yu V 1981 *JETP Lett.* **34** 272
Thornton T J, Pepper M, Ahmed H, Andrews D and Davies G J 1986 *Phys. Rev. Lett.* **56** 1198
Timp G, Chang A M, Cunningham J E, Chang T Y, Mankiewich P, Behringer R and Howard R E 1987 *Phys. Rev. Lett.* **58** 2814
Timp G, Chang A M, deVegvar P, Howard R E, Behringer R, Cunningham J E and Mankiewich P 1988 *Surf. Sci.* at press
Washburn S, Umbach C P, Laibowitz R B and Webb R A 1985 *Phys. Rev.* B **32** 1789
Washburn S and Webb R A 1986 *Adv. Phys.* **35** 375
Webb R A, Washburn S, Umbach C and Laibowitz R A 1985 *Phys. Rev. Lett.* **54** 2696